CZECH TECHNICAL UNIVERSITY IN PRAGUE

FACULTY OF NUCLEAR SCIENCES AND PHYSICAL ENGINEERING

Department of Physics

Spreading of the quantum walk as a wave phenomenon

DIPLOMA THESIS

Author: Bc. Iva Bezděková
Supervisor: Ing. Martin Štefaňák, PhD.
Consultant: prof. Ing. Igor Jex, DrSc.
Year: 2012

Prohlášení

Prohlašuji, že jsem tuto diplomovou práci vypracovala samostatně a výhradně s použitím uvedené literatury.

Nemám závažný důvod proti použití tohoto školního díla ve smyslu §60 Zákona č.121/2000 Sb., o právu autorském, o právech souvisejících s právem autorským a o změně některých zákonů (autorský zákon).

V Praze dne ....

Bc. Iva Bezděková

Acknowledgments

I would like to thank to my supervisor Ing. Martin Štefaňák for suggesting the topic, for his patience, countless hours of consultations and help. I would also like to thank to my consultant prof. Igor Jex for his support and usefull comments. Without them the work would never exist.

Title: Spreading of the quantum walk as a wave phenomenon

Specialization: Mathematical physics

Type of thesis: Diploma thesis

Supervisor: Ing. Martin Štefaňák, PhD., FNSPE CTU in Prague

Consultant: prof. Ing. Igor Jex, DrSc., FNSPE CTU in Prague

Abstract: We study the spreading of quantum walks as a wave phenomenon. We focus on the Grover walk where the particle has a non-zero probability of staying at the origin. This is called the localization effect. We present a generalization of the three-state Grover walk on a line and two generalizations of the Grover walk on the square lattice. Each generalization is given by a one-parameter family of coins which preserves the localization effect. We determine the velocities of the probability peaks in dependence on the coin parameter and investigate the asymptotic behavior of the probability peaks.

Key words: quantum walk, Grover matrix, localization effect, wave propagation, probability distribution, stationary phase approximation.

Název: Šíření kvantové procházky jako vlnový jev

Abstrakt: Studujeme šíření kvantových procházek ve spojitosti s jejich vlnovým chováním. Přitom se zaměřujeme na Groverovu procházku, kde částice zůstává v počátku s nenulovou pravděpodobností. Tato vlastnost se nazývá efekt lokalizace. Uvedeme jedno zobecnění pro Groverovu procházku na přímce o třech stavech a dvě zobecnění pro Groverovu procházku na čtvercové síti. Každé zobecnění tvoří jednoparametrická množina procházek, které zachovávají efekt lokalizace. Následně vyjádříme rychlosti pravděpodobnostních píků v závislosti na parametru procházky a vyšetříme jejich asymptotické chování.

Klíčová slova: kvantová procházka, Groverova matice, efekt lokalizace, šíření vlny, pravděpodobnostní rozdělení, metoda stacionární fáze.

Contents

Introduction

This work is an introduction to quantum walks on a line and on the square lattice. The work is focused on walks with Grover matrix as a coin operator. The Grover coin walk exhibits a localization efffet which makes them particularly interesting. We are interested in the spreading of the quantum walk as well as its long time behavior. Another objective of the work is to find the place where the particle has the highest probability to appear and calculate the velocity of the corresponding peak.

The first chapter concentrates on one dimensional quantum walks. First, we deal with two possible movements of the particle. Second, it describes the extension of the walk. Except the motion to the left or to the right, the possibility to stay on its current location is added. As a coin operator we use the Grover matrix. It ensures the localization effect. Further the velocities of the highest probability peaks are calculated.

The second chapter is focused on the generalization of the Grover walk on the line which preserves the localization effect. The generalization is done by adding a phase factor into the spectral decomposition of the Grover matrix. We find a one-parameter family of one-dimensional walks with three possible moves. We show, that the localization effect is preserved. At the end of the chapter we calculate the velocities of the highest probability peaks depending on the added phase factor.

Chapter three contains an introduction to the two-dimensional quantum walk. As in the one-dimensional case, we describe how to find the highest peaks and how to calculate their velocities. We find the velocities of the highest probability peaks and analyze their long time behavior. The value of the probability for the highest peaks decreases with an increasing number of steps. Using the method of stationary phase we give a possible explanation of this decrease. At the end of the chapter, we change the basis variables. It shows some other interesting properties of the walk.

Penultimate fourth chapter is focused on one generalization of the Grover walk in two dimensions. The generalization is based on the work of Inui *et.al* [6] and exhibits the localization effect. As in the previous chapters, we calculate the velocities of the highest probability peaks. Further we are interested in its behavior in dependence on the number of ssteps. We make a numerical simulations depicting the situation. The end of the chapter is dedicated to the change of the basis variables in which we can find another interesting properties of the walk.

The last chapter aims on the generalization of the two-dimensional Grover walk according to the model given in the second chapter. We find the one-parameter family of Grover walk, where the parameter is the added phase. Further we find the velocities of the highest probability peaks and how the walk spreads with increasing time. We report on a numerical simulation of the decreasing value of the highest probability peaks with increasing number of steps. To uncover other interesting features, we introduce new variables and present the propagation of the quantum walk wave-packet in terms of the group velocities. A summary of our results and an outlook is given in the conclusion.

Chapter 1

Quantum walk on a line

Quantum walk can thought as a generalization of a classical random walk. The simplest classical random walk is the walk, where a particle can move in each step to the left or to the right with a given probability. Generalization of the walk leads to the two-state quantum walk. The coin tossing is replaced by a coin. The coin operator for a two state walk is represented by a $U(2)$ matrix. In classical walk the coin is firstly tossed and afterwards the walker moves according to the tossing result. In analogy with that in quantum walk, first the coin operator is applied, which superposes possible movements of the walker. Then a shift operator, which moves the walker according to the resulting mixture of possible movements, is applied.

The Hilbert space of the quantum walk is given by the tensor product of two spaces

$$H = H_p \otimes H_C.$$

Here H_p is the position space

$$H_p = Span\{|m\rangle, m \in \mathbb{Z}\}.$$

Since the allowed movements of the quantum particle are to the left or to the right, the coin space H_C is two-dimensional and we can write

$$H_C = \mathbb{C}^2 = Span\{|L\rangle, |R\rangle\}.$$

Vectors $|L\rangle, |R\rangle$ forming the the standard basis of the coin space H_C correspond to the steps to the left and to the right.

Each single step of the walk is then realized by the propagator U which is given by

$$U = S(I_p \otimes C). \tag{1.1}$$

The coin operator C acts only on the coin space H_C. The displacement operator S acts on the tensor product H of both position and coin spaces and has the form

$$S = \sum_{m=-\infty}^{m=\infty} \left(|m-1\rangle\langle m| \otimes |L\rangle\langle L| + |m+1\rangle\langle m| \otimes |R\rangle\langle R| \right). \tag{1.2}$$

The operator I_p is the identity on the position space H_p.

Now we can show on an example how the walker propagates. The most studied walk is the one with the coin operator given by the Hadamard matrix

$$C = H = \frac{1}{\sqrt{2}} \left(\begin{array}{cc} 1 & 1 \\ 1 & -1 \end{array} \right), \tag{1.3}$$

so that we select H as our coin operator. Let us start our walk at the origin with the coin state going to the right or to the left. The initial state has the form

$$|\psi(0)\rangle = |0\rangle \otimes |R\rangle \tag{1.4}$$

or

$$|\psi(0)\rangle = |0\rangle \otimes |L\rangle. \tag{1.5}$$

The first step of the walk reads

$$|0\rangle \otimes |R\rangle \xrightarrow{H} \frac{1}{\sqrt{2}} |0\rangle \otimes (|L\rangle - |R\rangle) \xrightarrow{S} \frac{1}{\sqrt{2}} \left(|1\rangle \otimes |L\rangle - |-1\rangle |R\rangle \right), \tag{1.6}$$

alternatively for the second initial state

$$|0\rangle \otimes |L\rangle \xrightarrow{H} \frac{1}{\sqrt{2}} |0\rangle \otimes (|L\rangle + |R\rangle) \xrightarrow{S} \frac{1}{\sqrt{2}} \left(|1\rangle \otimes |L\rangle + |-1\rangle |R\rangle \right). \tag{1.7}$$

At time t, it means after t steps, the state vector reads

$$|\psi(t)\rangle = \sum_m |m\rangle \left(\psi_L(m,t) |L\rangle + \psi_R(m,t) |R\rangle \right) = U(t) |\psi(0)\rangle, \tag{1.8}$$

where $U(t)$ is a unitary propagator. The probability of finding the particle after t steps at the position m is then given by the square of the norm of the probability amplitudes vector

$$p(m,t) = \parallel \psi(m,t) \parallel^2 = |\psi_L(m,t)|^2 + |\psi_R(m,t)|^2. \tag{1.9}$$

We introduced the vector of probability amplitudes as

$$\psi(m,t) = (\psi_L(m,t), \psi_R(m,t))^T.$$

Moreover, the vector evolves in time as

$$\begin{aligned}\psi(m,t+1) &= \frac{1}{\sqrt{2}}\begin{pmatrix} 1 & 1 \\ 0 & 0 \end{pmatrix}\psi(m+1,t) + \frac{1}{\sqrt{2}}\begin{pmatrix} 0 & 0 \\ 1 & -1 \end{pmatrix}\psi(m-1,t) \\ &= H_L\psi(m+1,t) + H_R\psi(m-1,t). \qquad (1.10)\end{aligned}$$

Considerable simplification of the time evolution equation (1.8) can be achieved using the Fourier transformation. We switch from discrete position variable to the more convenient continuous momentum variable.

$$\tilde{\psi}(k,t) = \sum_{m\in\mathbb{Z}} e^{ikm}\psi(m,t), k \in (0, 2\pi). \qquad (1.11)$$

This step leads to the equation

$$\tilde{\psi}(k,t) = \tilde{U}(k)\tilde{\psi}(k,t-1) = \tilde{U}^t(k)\tilde{\psi}(k,0), \qquad (1.12)$$

where $\tilde{\psi}(k,0)$ stands for the Fourier transformation of the initial state. If the particle begins the walk at the origin, the initial state in the momentum representation remains unchanged and $\tilde{\psi}(k,0) = \psi(0,0) = \psi_0$. The time evolution operator is formed by

$$\tilde{U}(k) = \begin{pmatrix} e^{-ik} & 0 \\ 0 & e^{ik} \end{pmatrix} \cdot H, \qquad (1.13)$$

and since it is unitary, it can be rewritten as spectral decomposition with the power of t only for the eigenvalues. The resulting solution of the time evolution equation (1.12) can be written as

$$\tilde{\psi}(k,t) = \sum_{j=1}^{2} \lambda_j^t (v_j(k), \psi_0) v_j(k). \qquad (1.14)$$

Here λ_j are eigenvalues and $v_j(k)$ are eigenvectors of $\tilde{U}(k)$. It is suitable to consider the eigenvalues as an exponential with the phase dependent on the momentum variable k,

$$\lambda_j(k) = e^{i\omega_j(k)}. \qquad (1.15)$$

Performing the inverse Fourier transformation we obtain the solution in the position representation

$$\begin{aligned}\psi(m,t) &= \frac{1}{2\pi}\int_0^{2\pi} \tilde{\psi}(k,t)e^{-imk}dk \\ \psi(m,t) &= \frac{1}{2\pi}\sum_{j=1}^{2}\int_0^{2\pi} dk e^{i(\omega_j(k)t-mk)}(v_j(k),\psi_0)v_j(k). \qquad (1.16)\end{aligned}$$

1.1 Grover walk on a line and localization

In the previous text we have described the simplest walk in one dimension, the two-state walk. Now, except of the two allowed shifts, we add another one. This leads to the extension of the coin operator to a $U(3)$ matrix and the coin space to a $H_C = \mathbb{C}^3$. Let us add be the possibility for the particle to stay at its location. The coin Hilbert space is given by

$$H_C = \mathbb{C}^3 = Span\{|L\rangle, |S\rangle, |R\rangle\}.$$

The displacement operator also changes, the final form reads

$$S = \sum_{m=-\infty}^{\infty} \left(|m-1\rangle\langle m| \otimes |L\rangle\langle L| + |m\rangle\langle m| \otimes |S\rangle\langle S| + |m+1\rangle\langle m| \otimes |R\rangle\langle R|\right). \tag{1.17}$$

The vector of probability amplitudes gains the form

$$\psi(m,t) = (\psi_L(m,t), \psi_S(m,t), \psi_R(m,t))^T. \tag{1.18}$$

An interesting choice for the coin operator is the Grover matrix

$$C = G = \frac{1}{3}\begin{pmatrix} -1 & 2 & 2 \\ 2 & -1 & 2 \\ 2 & 2 & -1 \end{pmatrix}. \tag{1.19}$$

This is so because this matrix allows for the localization effect of the walk [1], which cannot occur in the two-state walk. The particle has, except of two dominant probability peaks traveling one to the left and one to the right with the increasing number of steps, another probability peak localized at the origin. The reason why the localization occurs is that the time evolution operator of the walk $\tilde{U}(k)$ has one eigenvalue independent of the momentum variable k. That eigenvalue is equal to one. The localizing peak is illustrated on Fig. (1.1).

1.1.1 Velocities of the probability peaks

After the Fourier transformation in the momentum representation we obtain 3×3 time evolution operator

$$\tilde{U}(k) = \begin{pmatrix} e^{-ik} & 0 & 0 \\ 0 & 1 & 0 \\ 0 & 0 & e^{ik} \end{pmatrix} \cdot G. \tag{1.20}$$

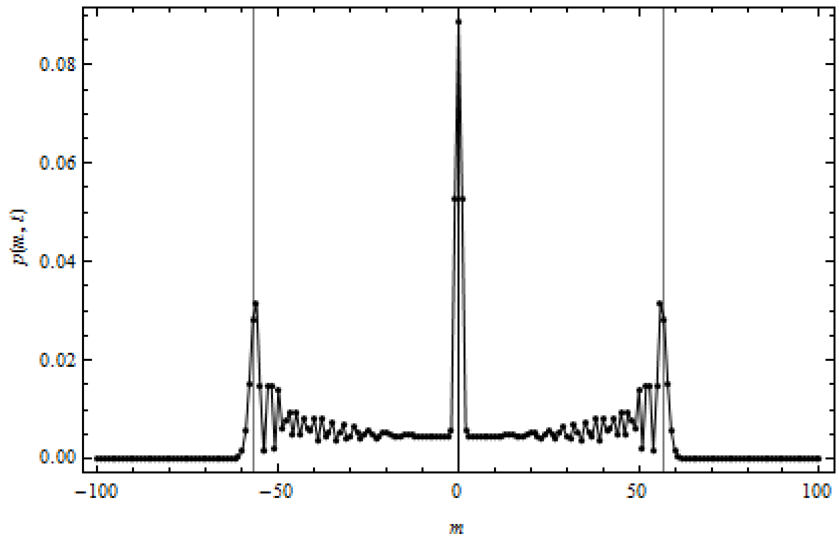

Figure 1.1: Probability distribution for the three-state quantum walk on a line with the Grover coin G after $t = 100$ and the initial state of the walk is $\psi_0 = (0, 1, 0)$. The vertical lines indicate the calculated location of the dominant peaks $m = v_{S,R,L} \cdot t$ where $v_S = 0$ and $v_{R,L} = \pm\frac{1}{\sqrt{3}}$.

The inverse Fourier transformation of the time evolution equation (1.14) leads us for the three-state walk to the equation

$$\psi(m,t) = \frac{1}{2\pi}\sum_{j=1}^{3}\int_0^{2\pi} dk e^{i(\omega_j(k)-\frac{m}{t}k)t}\left(v_j(k),\psi_0\right)v_j(k). \tag{1.21}$$

Square of norm of this integral gives us the probability of finding the particle at the position m at time t. The integral can be seen as an equation for the wave packet. Let us denote the phase as

$$\tilde{\omega}_j(k) = \omega_j(k) - \frac{m}{t}k. \tag{1.22}$$

Following the stationary phase theory (see [3], [4] or appendices) we know that the only significant contribution comes from the stationary points of $\tilde{\omega}_j(k)$. The main idea of the method relies on the cancellation of the increments to the integral, since the exponential is for large t a rapidly oscillating function. In the neighborhood of the stationary point of the phase factor, the exponential oscillates less rapidly and the cancellation less significant. Thus the flatness of the phase factor is crucial for the long time behavior. If $\tilde{\omega}_j(k)$ has no stationary point, the integration by parts gives that the integral (1.21) decays faster than any inverse power of t. If $\tilde{\omega}_j'(k_1) = 0$ than the integral decays proportional to $\frac{1}{\sqrt{t}}$. It gives us the inner part of the probability distribution. If $\tilde{\omega}_j'(k_2) = \tilde{\omega}_j''(k_2) = 0$, the integral decreases as $t^{-\frac{1}{3}}$. Such a point k_2 defines the highest probability peak.

First we have to find the phases of the eigenvalues, these are

$$\begin{aligned} \omega_{1,2}(k) &= \mp \arccos\left(-\frac{2+\cos k}{3}\right), \\ \omega_3(k) &= 0. \end{aligned} \tag{1.23}$$

Vanishing derivatives lead us to the set of equations for the first two eigenvalues

$$\begin{aligned} \frac{d\tilde{\omega}_{1,2}(k)}{dk} &= \frac{d\omega_{1,2}(k)}{dk} - \frac{m}{t} = \pm\frac{\sin k}{\sqrt{3-(2+\cos k)^2}} - v = 0, \\ \frac{d^2\tilde{\omega}_{1,2}(k)}{dk^2} &= \frac{d^2\omega_{1,2}(k)}{dk^2} = \mp\frac{8(\sin\frac{k}{2})^4}{((1-\cos k)(5+\cos k))^{\frac{3}{2}}} \\ &= \pm 2\sqrt{\frac{1-\cos k}{(5+\cos k)^3}} = 0. \end{aligned} \tag{1.24}$$

Equations for the third eigenvalue are simple

$$\begin{aligned} \frac{d\tilde{\omega}_3(k)}{dk} &= -\frac{m}{t} = 0 \\ \frac{d^2\tilde{\omega}_3(k)}{dk^2} &= 0. \end{aligned} \tag{1.25}$$

Let us first discuss the result for the nonzero phases $\omega_{1,2}(k)$. The second equation of (1.24) is satisfies for $k = 2\pi n, n \in \mathbb{Z}$. Provided that k ranges from 0 to 2π it means that the second derivative vanishes for

$$k_0 = 0. \tag{1.26}$$

The first equation from (1.24) gives the relation [2]

$$m = \frac{d\omega_{1,2}}{dk}(k_0)\cdot t = v\cdot t. \tag{1.27}$$

Thus we can assign the velocities to the peaks and using (1.26) they are equal to

$$\begin{aligned} v_L &= \lim_{k\to k_{0+}} \frac{d\omega_1}{dk}(k) = -\frac{1}{\sqrt{3}}, \\ v_R &= \lim_{k\to k_{0+}} \frac{d\omega_2}{dk}(k) = \frac{1}{\sqrt{3}}. \end{aligned} \tag{1.28}$$

The limit is needed because the first derivative of the phase ω_j in k_0 does not exist. Now we can easily see that the equations (1.25) corresponds to the non-traveling peak whose velocity

$$v_S = \frac{d\omega_3}{dk}(k) \cdot t = 0 \tag{1.29}$$

for an arbitrary $k \in (0, 2\pi)$.

In addition, we should point out the connection to the wave behavior. The relation (1.21) is similar to an equation for the spreading of the wave packet. The relation between the frequency of the motion and its wavenumber is called the dispersion relation. Consider our momentum k as this awe number and $\omega(k)$ as the frequency. Then the first derivative of the frequency $\omega(k)$ with respect to k determines the group velocity of spreading of the wave packet, $v = v_g = d\omega(k)/dk$ [9]. Thus here the group velocity for the three-state Grover walk is

$$\frac{d\omega_{1,2}(k)}{dk} = \pm \frac{\sin k}{\sqrt{3 - (2 + \cos k)^2}} = v.$$

Chapter 2

Generalized Grover walk on a line

Let us consider the Grover matrix. We know that the Grover walk exhibits the localization effect. The question is, if there exist any other coins or even any family of coins preserving the localization effect as well. In [7] it was shown that such a family of coins exists.

The symmetry of the Grover matrix is such that any permutation of the basis states does not change it. Thus we can find the shared eigenvalues of the Grover matrix G and some permutation matrix P_G. One eigenvalue of P_G and G corresponding to the shared eigenvector differ by sign. The remaining two eigenvalues are the same for both matrices. Adding a phase factor into the spectral decomposition of G switches between these two sign, i.e. it switches between the Grover and the permutation matrix. The only adequate 3×3 permutation matrix is

$$P_g = \begin{pmatrix} 0 & 0 & 1 \\ 0 & 1 & 0 \\ 1 & 0 & 0 \end{pmatrix}. \tag{2.1}$$

Consider the orthonormal basis formed by the shared eigenvectors of G and P_G

$$\begin{aligned} v_1 &= \frac{1}{\sqrt{2}}(-1, 0, -1)^T, \\ v_2 &= \frac{1}{\sqrt{6}}(-1, 2, -1)^T, \\ v_3 &= \frac{1}{\sqrt{3}}(1, 1, 1)^T. \end{aligned} \tag{2.2}$$

The relevant eigenvalues are

$$\begin{aligned} \lambda^G_{1,2,3} &= -1,-1,1 \\ \lambda^{P_G}_{1,2,3} &= -1,1,1. \end{aligned} \tag{2.3}$$

As we see, $\lambda^G_2 = -\lambda^{P_G}_2$. For the original Grover matrix hold

$$G = -v_1^T \cdot v_1 - v_2^T \cdot v_2 + v_3^T \cdot v_3. \tag{2.4}$$

To switch between the eigenvalues $\lambda^G_2 \leftrightarrow \lambda^{P_G}_2$ we have to add a phase factor e^{ic} in front of the second member of the spectral decomposition

$$\begin{aligned} G(c) &= -v_1^T \cdot v_1 - e^{ic} v_2^T \cdot v_2 + v_3^T \cdot v_3 \\ &= \frac{1}{6}\begin{pmatrix} -1-e^{ic} & 2(1+e^{ic}) & 5-e^{ic} \\ 2(1+e^{ic}) & 2(1-2e^{ic}) & 2(1+e^{ic}) \\ 5-e^{ic} & 2(1+e^{ic}) & -1-e^{ic} \end{pmatrix}. \end{aligned} \tag{2.5}$$

The choice of the phase $c = 0$ leads to the original Grover coin. On the other hand, the choice of the phase $c = \pi$ gives the permutation matrix

$$G(\pi) = \begin{pmatrix} 0 & 0 & 1 \\ 0 & 1 & 0 \\ 1 & 0 & 0 \end{pmatrix}. \tag{2.6}$$

As will be shown later, this one-parameter family of coins preserves the constant eigenvalue of the time evolution operator $\tilde{U}(k,c)$.

2.1 Velocities of the probability peaks

In this section we will determine the velocities of the highest probability peaks of finding the particle. The time evolution operator for the one parameter family of walks has the form

$$\tilde{U}(k,c) = \begin{pmatrix} e^{-ik} & 0 & 0 \\ 0 & 1 & 0 \\ 0 & 0 & e^{ik} \end{pmatrix} \cdot G(c). \tag{2.7}$$

For its eigenvalues $e^{i\omega_j(k,c)}$

$$\begin{aligned} \omega_{1,2}(k,c) &= \frac{c}{2} \pm \arccos\left(\frac{1}{3}\cos\left(\frac{c}{2}\right)(2+\cos k)\right), \\ \omega_3(k,c) &= 0. \end{aligned} \tag{2.8}$$

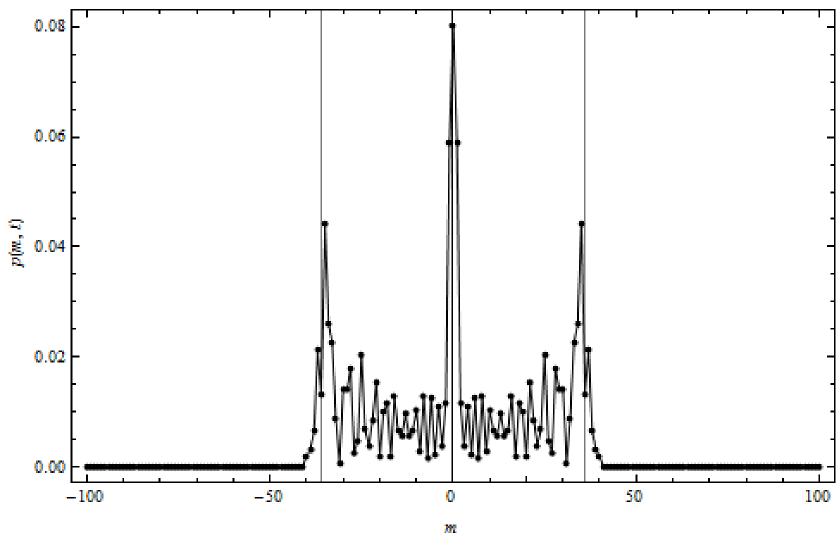

Figure 2.1: The probability distribution for the three-state quantum walk on a line with Grover coin $G(c)$, $G(\frac{\pi}{3})$. The number of steps is $t = 100$ and the initial state of the walk is $\psi_0 = (0, 1, 0)$. The vertical lines correspond to the calculated locations of the highest peaks $m(c) = v(c) \cdot t$ where $v_S(c) = 0$ and $v_{R,L}(c) \approx \pm \frac{1}{\sqrt{3}}(1 - \frac{c}{\pi})$.

As we can see, one eigenvalue is as in the Grover walk independent of the momentum k. Thus there exists a probability peak with zero velocity.

For the two remaining eigenvalues we have to evaluate the appropriate velocities of the peaks. The first and the second derivatives of $\tilde{\omega}_{1,2}(k,c) = \omega_{1,2}(k,c) - \frac{m}{t}k$ are

$$\begin{aligned}
\frac{d\tilde{\omega}_{1,2}(k,c)}{dk} &= \frac{d\omega_{1,2}(k,c)}{dk} - \frac{m}{t} = \pm\frac{\cos\frac{c}{2}\sin k}{\sqrt{9-(\cos\frac{c}{2}(2+\cos k))^2}} - v, \\
\frac{d^2\tilde{\omega}_{1,2}(k,c)}{dk^2} &= \frac{d^2\omega_{1,2}(k,c)}{dk^2} = \pm\frac{\cos\frac{c}{2}(9\cos k - \cos^2\frac{c}{2}(3+5\cos k+\cos 2k))}{(9-\cos^2\frac{c}{2}(2+\cos k)^2)^{3/2}}.
\end{aligned} \tag{2.9}$$

Both second derivatives vanish for

$$k_0 = 2\arccos\left(\frac{9-5\cos^2\frac{c}{2} - 3\sin\frac{c}{2}\sqrt{9-\cos^2\frac{c}{2}}}{4\cos^2\frac{c}{2}}\right). \tag{2.10}$$

The group velocity of the walk is

$$\frac{d\omega_1}{dk}(k,c) = -\frac{\cos\frac{c}{2}\sin\frac{c}{2}}{\sqrt{9-\cos^2\frac{c}{2}(2+\cos k)^2}} = v(k,c) \tag{2.11}$$

and for the highest right and the left traveling peaks

$$\begin{aligned}
v_L(c) &= \frac{d\omega_1}{dk}(k_0,c) = -\sqrt{\frac{3-\cos^2\frac{c}{2} - \sin\frac{c}{2}\sqrt{9-\cos\frac{c}{2}}}{6}}, \\
v_R(c) &= \frac{d\omega_2}{dk}(k_0,c) = -v_L(c).
\end{aligned} \tag{2.12}$$

Acquired velocities dependent on a phase c are displayed on figure (2.1). As we can see, the dependence is almost linear

$$v_R(c) = -v_L(c) \approx \frac{1}{\sqrt{3}}\left(1-\frac{c}{\pi}\right). \tag{2.13}$$

Further we find that from the one-parameter family of coins $G(c)$ the original Grover walk with $G = G(0)$ is the fastest one. With increasing phase c the walk slows down until its velocity becomes zero for the phase $c = \pi$, i.e $v_R(\pi) = 0$.

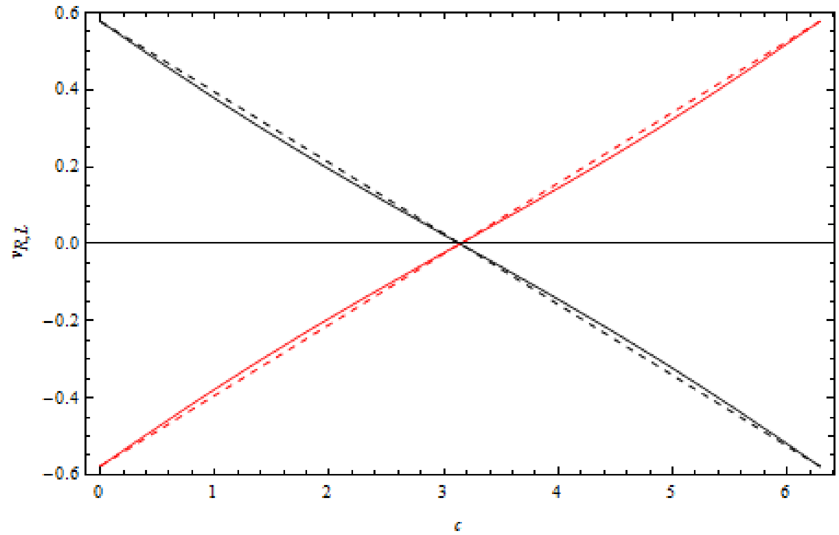

Figure 2.2: Dependence of the highest probability peaks velocities (2.12) for the Grover walk with phase $G(c)$ on its phase c. Moreover, we show the difference between the velocities and their linear approximations $v_{R,L} \approx \pm\frac{1}{\sqrt{3}}(1-\frac{c}{\pi})$. Velocity of the right (left) traveling peak is plotted by black (red) full line and its approximation by black (red) dashed line.

Chapter 3

Grover walk on a square lattice

Let us extend the quantum walk on the line into the second dimension. Instead of the line, the walk is now realized on the square lattice. In the classical case one can imagine the walk on the square network as two connected walks on the line. First, we decide which line to choose, horizontal or vertical. Second, we move on the selected one according to the coin tossing. In the quantum case, the coin operator mixes the states of both lattices into a superposition of the basis states of the coin space.

As in the one-dimensional case, the walk takes place in the Hilbert space given by the tensor product of position and coin space $H = H_P \otimes H_C$. The particle has four possible movements, they are to the left, right, down or up. Thus for the coin space holds

$$H_C = \mathbb{C}^4 = span\{|L\rangle, |R\rangle, |D\rangle, |U\rangle\}.$$

The position space H_P is now given by the tensor product of two one-dimensional position spaces

$$H_P = span\{|m_1, m_2\rangle \ ; m_{1,2} \in \mathbb{Z}\},$$

where $'m_1'$ belongs to the position on the horizontal lattice, i.e. to the move to the left or to the right and $'m_2'$ belongs to the position on the vertical lattice, i.e. to the move up or down.

Each single step is given by (1.1), nevertheless the shift operator S changes to

$$
\begin{aligned}
S &= \sum_{m,n=-\infty}^{\infty} (|m-1,n\rangle\langle m,n| \otimes |L\rangle\langle L| + |m+1,n\rangle\langle m,n| \otimes |R\rangle\langle R| \\
&+ |m,n-1\rangle\langle m,n| \otimes |D\rangle\langle D| + |m,n+1\rangle\langle m,n| \otimes |U\rangle\langle U|).
\end{aligned} \tag{3.1}
$$

The coin operator C is a $U(4)$ matrix. Subsequent description of the walk is analogical to the one-dimensional case, thus we mention it only briefly. The wave function or the vector of probability amplitudes on the coordinate $\vec{m} = (m_1, m_2)$ at time t is composed of four components

$$
\psi(\vec{m}, t) = (\psi_L(\vec{m}, t), \psi_R(\vec{m}, t), \psi_D(\vec{m}, t), \psi_U(\vec{m}, t))^T. \tag{3.2}
$$

In this case there exists a coin leading to the localization effect. It is a four-dimensional Grover coin. The localizing Grover coin can be constructed for each higher dimension as follows. Let the state $|x\rangle$ denote the uniform superposition over all states of the standard basis of some Hilbert space

$$
|x\rangle = \frac{1}{\sqrt{N}} \sum_{i=1}^{N} |i\rangle, \tag{3.3}
$$

where N is the dimension of the space. Then the operator

$$
G_N = 2|x\rangle\langle x| - I = \frac{2}{N} \begin{pmatrix} 1 & 1 & 1 & . & . \\ 1 & 1 & 1 & . & . \\ 1 & 1 & 1 & . & . \\ . & . & . & . & \\ . & . & . & & . \end{pmatrix} - I,
$$

is the n-dimensional Grover matrix.

Consider as a coin operator the four-dimensional Grover matrix

$$
G_4 = \frac{1}{2} \begin{pmatrix} -1 & 1 & 1 & 1 \\ 1 & -1 & 1 & 1 \\ 1 & 1 & -1 & 1 \\ 1 & 1 & 1 & -1 \end{pmatrix}. \tag{3.4}
$$

The time evolution of the walk is

$$\begin{aligned}\psi(\vec{m},t)=\psi(m_1,m_2,t+1) &= G_{4_L}\psi(m_1+1,m_2,t)+G_{4_R}\psi(m_1-1,m_2,t)\\ &+ G_{4_D}\psi(m_1,m_2+1,t)+G_{4_U}\psi(m_1,m_2-1,t),\end{aligned}\tag{3.5}$$

where

$$G_{4_L}=\frac{1}{2}\begin{pmatrix}-1&1&1&1\\0&0&0&0\\0&0&0&0\\0&0&0&0\end{pmatrix}, G_{4_R}=\frac{1}{2}\begin{pmatrix}0&0&0&0\\1&-1&1&1\\0&0&0&0\\0&0&0&0\end{pmatrix},$$

$$G_{4_D}=\frac{1}{2}\begin{pmatrix}0&0&0&0\\0&0&0&0\\1&1&-1&1\\0&0&0&0\end{pmatrix}, G_{4_U}=\frac{1}{2}\begin{pmatrix}0&0&0&0\\0&0&0&0\\0&0&0&0\\1&1&1&-1\end{pmatrix}.\tag{3.6}$$

The Fourier transformation

$$\tilde{\psi}(\vec{k},t)=\tilde{\psi}(k_1,k_2,t)=\sum_{\vec{m}\in Z^2}\psi(\vec{m},t)e^{ik_1t}e^{ik_2t},\tag{3.7}$$

transforms the time evolution equation from the position representation into the momentum representation. The vector is $\vec{k}=(k_1,k_2)$ and both $k_{1,2}$ ranges from $-\pi$ to π. The time evolution equation acquires the simplified form

$$\tilde{\psi}(\vec{k},t)=\tilde{U}(\vec{k})\tilde{\psi}(\vec{k},t-1)=\tilde{U}^t(\vec{k})\tilde{\psi}(\vec{k},0),\tag{3.8}$$

and the time evolution operator in the momentum representation is given by

$$\begin{aligned}\tilde{U}(\vec{k}) &= \frac{1}{2}\begin{pmatrix}-e^{-ik_1}&e^{-ik_1}&e^{-ik_1}&e^{-ik_1}\\e^{ik_1}&-e^{ik_1}&e^{ik_1}&e^{ik_1}\\e^{-ik_2}&e^{-ik_2}&-e^{-ik_2}&e^{-ik_2}\\e^{ik_2}&e^{ik_2}&e^{ik_2}&-e^{ik_2}\end{pmatrix}\\ &= \begin{pmatrix}e^{-ik_1}&0&0&0\\0&e^{ik_1}&0&0\\0&0&e^{-ik_2}&0\\0&0&0&e^{ik_2}\end{pmatrix}\cdot G_4.\end{aligned}\tag{3.9}$$

The initial state in the Fourier picture is equal to the initial state in position domain provided that the walk starts from the origin, $\tilde{\psi}(\vec{k},0)=\psi(0,0,0)=\psi_0$. The spectral decomposition of the time evolution operator $\tilde{U}(\vec{k})$ and subsequent inverse Fourier transformation allows us to write the resulting form of the wave function in position representation in the form

$$\psi(\vec{m},t)=\frac{1}{(2\pi)^2}\sum_{j=1}^{4}\int_{-\pi}^{\pi}dk_1\int_{-\pi}^{\pi}dk_2 e^{i(\omega_j(\vec{k})-\frac{\vec{m}\cdot\vec{k}}{t})t}(v_j(\vec{k}),\psi_0)v_j(\vec{k}), \tag{3.10}$$

where $j\in\{1,2,3,4\}$.

3.1 Velocities of the probability peaks

Analogously to the one-dimensional walk, we would like to determine the velocities of the probability peaks. Using the same procedure as in the previous sections we obtain the velocities of the highest peaks. The equation (3.10) is now the generalized equation of the wave packet in two dimensions describing its propagation. We can generalize the relation for the group velocity (1.27) in a straightforward way as the gradient of the frequency

$$\vec{v}=\nabla_{\vec{k}}\omega(\vec{k}). \tag{3.11}$$

We are looking for the velocities of the dominant peaks. These peaks occur at the coordinates (m_1,m_2) where the integral (3.10) contributes the most. Following the method of stationary phase the group velocity of the highest peaks will be found in such a point $\vec{k}=\vec{k_0}$, where $\tilde{\omega}_j(\vec{k})=\omega_j(\vec{k})-\frac{\vec{m}\cdot\vec{k}}{t}$ in the (3.10) has vanishing the first derivative with respect to $\vec{k}$. As for the second derivatives the Hessian matrix should be singular.

The eigenvalues of the propagator (3.9) are $e^{i\omega_j(\vec{k})}$ and the frequencies read

$$\begin{aligned}\omega_{1,2}(\vec{k}) &= \mp\arccos\left(-\frac{1}{2}(\cos k_1+\cos k_2)\right),\\ \omega_{3,4}(\vec{k}) &= 0.\end{aligned} \tag{3.12}$$

Zero-valued frequencies lead to the stationary probability peak, thus for one velocity

$$\vec{v}_s=\vec{0}. \tag{3.13}$$

To find $\vec{k}_0$ we have to determine when the Hessian matrix

$$H(\omega_j(\vec{k})) = \begin{pmatrix} \frac{d^2\omega_j(\vec{k})}{d^2k_1} & \frac{d^2\omega_j(\vec{k})}{dk_1dk_2} \\ \frac{d^2\omega_j(\vec{k})}{dk_2dk_1} & \frac{d^2\omega_j(\vec{k})}{d^2k_2} \end{pmatrix} \tag{3.14}$$

is singular. The second derivatives of the frequencies (3.12) are

$$\begin{aligned} \frac{\partial^2\omega_1(\vec{k})}{\partial^2k_1} &= \frac{\partial^2\omega_2(\vec{k})}{\partial^2k_1} = -\frac{(1+\cos^2 k_1)\cos k_2 + (-3+\cos^2 k_2)\cos k_1}{[(2-(\cos k_1+\cos k_2))(2+\cos k_1+\cos k_2)]^{3/2}}, \\ \frac{\partial^2\omega_1(\vec{k})}{\partial^2k_2} &= \frac{\partial^2\omega_2(\vec{k})}{\partial^2k_2} = -\frac{(1+\cos^2 k_2)\cos k_1 + (-3+\cos^2 k_1)\cos k_2}{[(2-(\cos k_1+\cos k_2))(2+\cos k_1+\cos k_2)]^{3/2}}, \\ \frac{\partial^2\omega_{1,2}(\vec{k})}{\partial k_1\partial k_2} &= \frac{\partial^2\omega_{1,2}(\vec{k})}{\partial k_2\partial k_1} = -\frac{(\cos k_1+\cos k_2)\sin k_1\sin k_2}{[(2-(\cos k_1+\cos k_2))(2+\cos k_1+\cos k_2)]^{3/2}}. \end{aligned} \tag{3.15}$$

We solve the equation

$$\det H(\omega_j(\vec{k})) = 0, \tag{3.16}$$

where

$$\det H(\omega_j) = \frac{(\cos k_1 - \cos k_2)^2}{(-2+\cos k_1+\cos k_2)^2(2+\cos k_1+\cos k_2)^2}. \tag{3.17}$$

It is satisfied for

$$k_1 = \pm k_2. \tag{3.18}$$

Thus

$$\vec{k}_0 = (k_1, \pm k_1), \tag{3.19}$$

and $k_{1,2}$ ranges between $(-\pi,\pi)$.

Due to the equation (3.11) the velocity of the particle with momentum $\vec{k}$ is given by

$$\vec{v}(\vec{k}) = (v_1^{(\pm)}(\vec{k}), v_2^{(\pm)}(\vec{k})) = \left(\frac{\partial\omega_j}{\partial k_1}(\vec{k}), \frac{\partial\omega_j}{\partial k_2}(\vec{k})\right), \quad j \in 1,2 \tag{3.20}$$

where

$$\begin{aligned} \frac{\partial\omega_{1,2}(\vec{k})}{\partial k_1} &= \pm\frac{\sin k_1}{\sqrt{(2-(\cos k_1+\cos k_2))(2+\cos k_1+\cos k_2)}} = v_1^{(\pm)}(\vec{k}), \\ \frac{\partial\omega_{1,2}(\vec{k})}{\partial k_2} &= \pm\frac{\sin k_2}{\sqrt{(2-(\cos k_1+\cos k_2))(2+\cos k_1+\cos k_2)}} = v_2^{(\pm)}(\vec{k}). \end{aligned} \tag{3.21}$$

and for the highest peaks

$$\vec{v}^{HP} = (v_1^{HP}, v_2^{HP}) = \left(\frac{d\omega_j}{dk_1}(\vec{k}_0), \frac{d\omega_j}{dk_2}(\vec{k}_0)\right), \tag{3.22}$$

The velocities of the highest moving peaks

$$\begin{aligned}
\vec{v}_1^{HP} &= \left(\ \frac{1}{2}, \ \ \frac{1}{2}\right), \\
\vec{v}_2^{HP} &= \left(-\frac{1}{2}, \ \ \frac{1}{2}\right), \\
\vec{v}_3^{HP} &= \left(-\frac{1}{2}, -\frac{1}{2}\right), \\
\vec{v}_4^{HP} &= \left(\ \frac{1}{2}, -\frac{1}{2}\right).
\end{aligned} \tag{3.23}$$

This result for the highest peaks belongs to such a $\vec{k}_0$, where the Hessian matrix is singular, but non-zero. Its rank is equal to one. From the numerical simulation in the Fig. (3.1) we see that except the four highest peaks there is also high probability of finding the particle on the border of the non-zero part of the probability distribution. It should be noted that the range of the velocities (3.21) form a circle

$$v_1^2 + v_2^2 \leq \frac{1}{2}. \tag{3.24}$$

One might think that the velocities on the boarder, where $v_1^2 + v_2^2 = 1/2$, correspond also to the singular Hessian matrix. Nevertheless solving the zero-valued determinant of $H(\omega_j)$ does not give such velocities. Moreover, as we will show later, the second derivatives on the circle $v_1^2 + v_2^2 = 1/2$ are not defined. The rank of the Hessian matrix is equal to one on condition $k_1 = \pm k_2$, but it leads only to the velocities (3.23).

3.2 Decrease of the highest probability peaks

According to the method of the stationary phase [3], [4], we can predict decreasing behavior of the highest probability peaks depending on the type of the stationary point of the phase $\tilde{\omega}_j$.

As we can see from the numerical simulation in the Fig. (3.2), maximal peaks of the probability distribution (3.1) decrease as an inverse value of the total

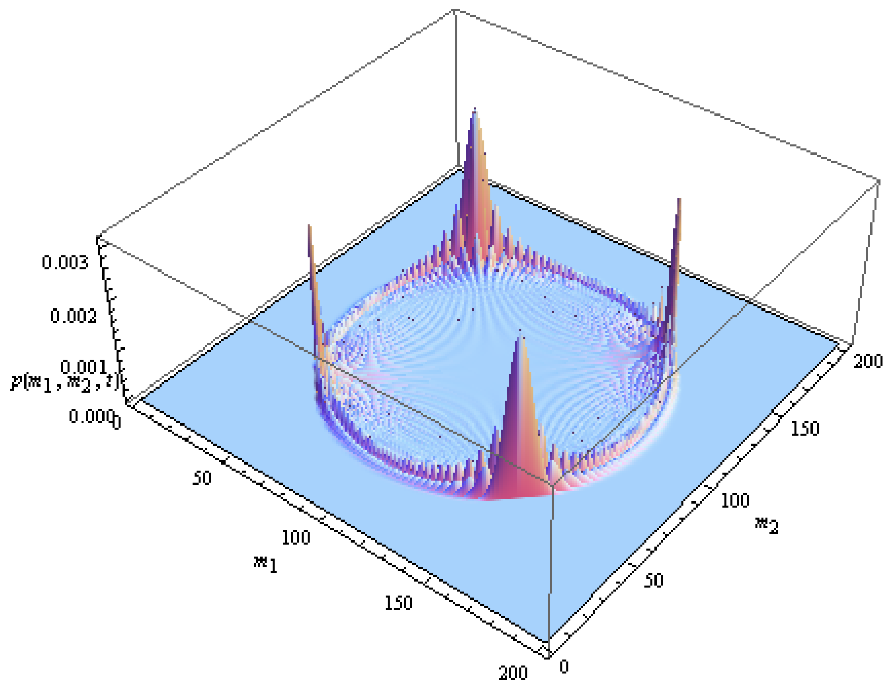

Figure 3.1: Probability distribution for the quantum walk on a square lattice with Grover coin G_4. The number of steps is $t = 100$ and the initial state of the walk is $\psi_0 = \frac{1}{2}(1, 1, -1, -1)$. Using this initial state, the localization disappears. The highest peaks travel with constant velocities $\vec{v} = (\pm\frac{1}{2}, \pm\frac{1}{2})$.

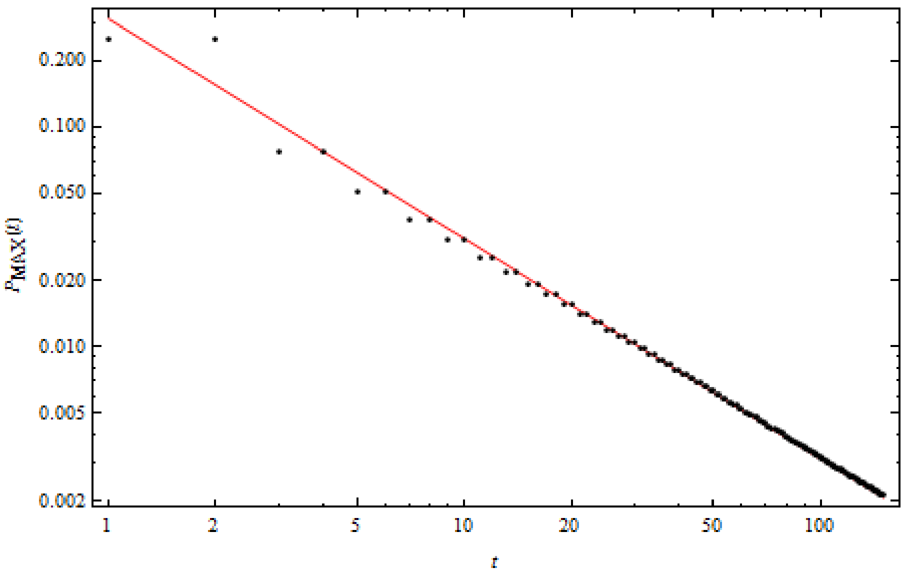

Figure 3.2: Logarithmic plot illustrating the decrease off the value of the highest probability peaks in (3.1) dependence on the number of steps t by black, in comparison with its inverse value t^{-1} by red. The initial state of the walk is $\psi_0 = \frac{1}{2}(1, 1, -1, -1)$. The total number of steps t on the x axis goes from 0 to 150. On the y axis is plotted maximal probability of finding the particle i.e. the value of the highest peak in the probability distribution after t steps. For the large number of steps the value of the highest probability peaks decrease as an inverse value of m. This property follows from the stationary phase approximation, since the stationary points of the phase $\tilde{\omega}_j = \omega_j - \vec{v} \cdot \vec{k}$ form a curve.

number of steps t i.e. t^{-1}. Such a decrease occurs if the stationary points of the phase $\tilde{\omega}_j$ form a curve (see Chap.9 in [3] or Appendices). The curve is formed by points $k_1 = \pm k_2$. The situation is illustrated on Fig. (3.3).

3.3 Change of the basis variables

Some properties of the walks can be found by changing the momentum variables $\vec{k} = (k_1, k_2)$ to the velocities $\vec{v} = (v_1, v_2)$. This mapping is one-to-two (see for example figure (3.3)).

Let us consider the Grover walk. Using $v_{1,2}^{(\pm)}(\vec{k}, p)$ from equation (3.21) we find momentum variables as a function of the velocities. It is sufficient to consider only one of the velocities, for instance $v_{1,2}^{(+)}(\vec{k}, p)$. Let us denote $v_{1,2}^{(+)}(\vec{k}, p) = v_1$. The resulting relation are

$$
\begin{aligned}
\sin k_1 &= \frac{2v_1\sqrt{1-2(v_1^2+v_2^2)}}{\sqrt{(v_1+v_2+1)(v_1-v_2+1)(v_1+v_2-1)(v_1-v_2-1)}}, \\
\cos k_1 &= \frac{3v_1^2+v_2^2-1}{\sqrt{(v_1+v_2+1)(v_1-v_2+1)(v_1+v_2-1)(v_1-v_2-1)}}, \\
\sin k_2 &= \frac{2v_2\sqrt{1-2(v_1^2+v_2^2)}}{\sqrt{(v_1+v_2+1)(v_1-v_2+1)(v_1+v_2-1)(v_1-v_2-1)}}, \\
\cos k_2 &= -\frac{v_1^2+3v_2^2-1}{\sqrt{(v_1+v_2+1)(v_1-v_2+1)(v_1+v_2-1)(v_1-v_2-1)}}.
\end{aligned}
\tag{3.25}
$$

The determinant of the Hessian matrix equals in the original momentum variables equal to

$$
\det H(\omega_j) \quad = \quad \frac{(\cos k_1 - \cos k_2)^2}{(-2+\cos k_1+\cos k_2)^2(2+\cos k_1+\cos k_2)^2}
$$

and the derivatives of the frequencies $\omega_j,\ j \in \{1, 2\}$ are from equation (3.15). We were interested in such $k_{1,2}$, where the Hessian matrix is singular. The transformation to the velocity variables gives

$$
\det H(\omega_j) = -\frac{1}{4}(v_1+v_2+1)(v_1-v_2+1)(v_1+v_2-1)(v_1-v_2-1). \tag{3.26}
$$

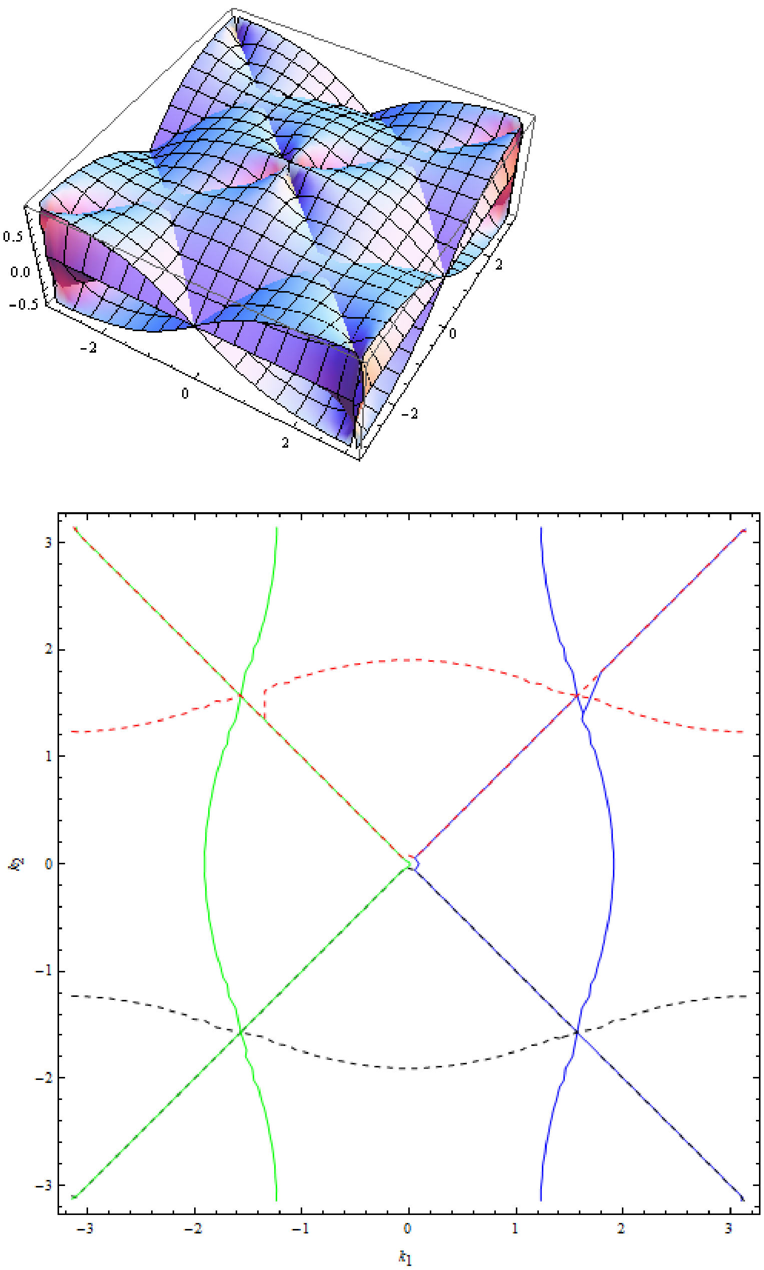

Figure 3.3: Contours lines giving the velocities $v_{1,2}^{(\pm)}(\vec{k})$ in both directions (3.21) equal to $\frac{1}{2}$. The curve of stationary points is formed by $k_1 = \pm k_2$ and illustrated by mixing solid lines with dashed lines. Blue and green line correspond to the $v_1^{(\pm)}(\vec{k}) = \frac{1}{2}$, red and black dashed line corresponds to the $v_2^{(\pm)}(\vec{k}) = \frac{1}{2}$. Top figure shows the velocities $v_{1,2}^{(\pm)}(\vec{k})$ from (3.21) and is well seen that contour plot cuts this figure at the velocity $\frac{1}{2}$.

Thus the matrix is singular only if

$$\begin{aligned} |v1 + v_2| &= 1 \\ |v1 - v_2| &= 1. \end{aligned} \tag{3.27}$$

Considering the region covered by the walk, the only reasonable result is that the matrix is singular for

$$v_{1,2} = \pm\frac{1}{2}. \tag{3.28}$$

It is equivalent to the velocities of the highest peak and corresponds to the results obtained in the momentum variable (3.23). The situation is illustrated in the Fig. (3.3). The walk covers the points of the circle. We can try to explain, why there does not exist any velocities that gives the singular Hessian matrix and correspond to the smaller peaks of the walk. The smaller peaks are located on the boarder of the walk region where $v_1^2 + v_2^2 = \frac{1}{2}$. The second derivatives of the frequencies from equation (3.15) can be using (3.25) transfered into the new variables as

$$\begin{aligned} \frac{\partial^2\omega_{1,2}}{\partial^2 k_1} &= \frac{-1 + v_2^2 + v_1^2(3 + 2v_2^2 - 2v_1^2)}{\sqrt{2}\sqrt{\frac{1}{2} - v_1^2 - v_2^2}}, \\ \frac{\partial^2\omega_{1,2}}{\partial k_1 \partial k_2} &= \frac{v_1 v_2 (v_2^2 - v_1^2)}{\sqrt{2}\sqrt{\frac{1}{2} - v_1^2 - v_2^2}}, \\ \frac{\partial^2\omega_{1,2}}{\partial^2 k_2} &= -\frac{-1 + v_1^2 + v_2^2(3 + 2v_1^2 - 2v_2^2)}{\sqrt{2}\sqrt{\frac{1}{2} - v_1^2 - v_2^2}}. \end{aligned} \tag{3.29}$$

Also for the smaller peaks (where $\frac{1}{2} - v_1^2 - v_2^2 = 0$) the second derivatives do not exist.

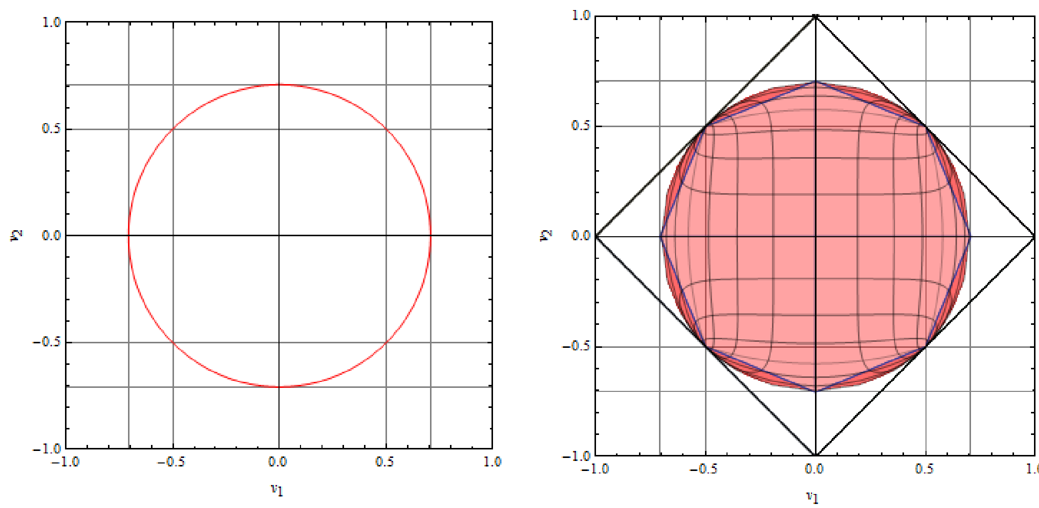

Figure 3.4: Parametric figure of the velocities $v_{1,2}^{(\pm)}(\vec{k})$ from equation (3.21) on the right. The thick black lines correspond to the singular Hessian matrix in the velocity variable (equation (3.26)). The grid lines in the position $v_{1,2} = \pm\frac{1}{2}$ depict the velocities of the highest peaks and $\pm\frac{1}{\sqrt{2}}$ depict the maximal velocities in each direction. The thick black lines touch the velocity region in the points belonging to the velocities of the highest probability peaks. The left figure illustrates the boundary of the velocity region with the grid lines in the same positions.

Chapter 4

Generalized Grover walk on a square lattice with parameter p

In [6] Inui *et al.* introduced a one-parameter family of quantum coins as a generalization of the Grover coin. It is

$$G(p) = \begin{pmatrix} -p & q & \sqrt{pq} & \sqrt{pq} \\ q & -p & \sqrt{pq} & \sqrt{pq} \\ \sqrt{pq} & \sqrt{pq} & -q & p \\ \sqrt{pq} & \sqrt{pq} & p & -q \end{pmatrix}, \quad p + q = 1 \tag{4.1}$$

and

$$p, q \in (0, 1).$$

The special case $p = \frac{1}{2}$ results in the Grover walk.

The time evolution operator in the momentum variables $\vec{k} = (k_1, k_2)$ is given by

$$\tilde{U}(\vec{k}, p) = \begin{pmatrix} e^{-ik_1} & 0 & 0 & 0 \\ 0 & e^{ik_1} & 0 & 0 \\ 0 & 0 & e^{-ik_2} & 0 \\ 0 & 0 & 0 & e^{ik_2} \end{pmatrix} \cdot G(p). \tag{4.2}$$

As the evolution operator for the original Grover walk, it also has eigenvalues independent of the wavenumbers k_1, k_2. The eigenvalues are

$$\lambda_{1,2} = e^{i\omega_{1,2}(k_1,k_2,p)}, \quad \lambda_{3,4} = \pm 1.$$

The behavior of this generalized Grover walk was studied in [5].The authors have determined pseudovelocity of the particle and studied its long-time behavior depending on the parameter p of the quantum coin and the initial state of the walk. In the following sections we will focus on the properties of the highest peaks in the probability distribution. We show that their velocities and decay rates can be obtained in a similar way as for the Grover walk.

4.1 Velocities of the highest probability peaks

To find the velocities of the highest probability peaks for the generalized type of Grover walk in two dimensions we need to find the frequencies $\omega_j(\vec{k},p)$ belonging to the eigenvalues $\lambda_j = e^{i\omega_j(\vec{k},p)}$ of the time evolution operator (4.2). Note that $\lambda_{3,4} = \pm 1$, i.e. $\omega_{3,4} = 0$, indicate the existence of the central peak with zero velocity, $\vec{v}_S = \vec{0}$. The remaining frequencies are

$$\omega_{1,2}(\vec{k},p) = \mp \arccos\left(-(p\cos k_1 + q\cos k_2)\right), \quad q = 1-p. \tag{4.3}$$

The group velocity of the walk is given by the gradient of frequency with respect to the wave vector $\vec{k}$

$$\vec{v} = (v_1^{(\pm)_p}, v_2^{(\pm)_p}) = \left(\frac{\partial \omega_j}{\partial k_1}(\vec{k},p), \frac{\partial \omega_j}{\partial k_2}(\vec{k},p)\right)$$

and

$$\begin{aligned} v_1^{(\pm)_p} &= \pm\frac{p\sin k_1}{\sqrt{(1-(p\cos k_1 + q\cos k_2))(1+p\cos k_1 + q\cos k_2)}}, \\ v_2^{(\pm)_p} &= \pm\frac{q\sin k_2}{\sqrt{(1-(p\cos k_1 + q\cos k_2))(1+p\cos k_1 + q\cos k_2)}}, \quad q = 1-p. \end{aligned} \tag{4.4}$$

The search for the velocities of the highest peaks requires solving the equation for the singular non-zero Hessian matrix

$$H(\omega_j(\vec{k},p)) = \begin{pmatrix} \frac{d^2\omega_j(\vec{k},p)}{d^2k_1} & \frac{d^2\omega_j(\vec{k},p)}{dk_1 dk_2} \\ \frac{d^2\omega_j(\vec{k},p)}{dk_2 dk_1} & \frac{d^2\omega_j(\vec{k},p)}{d^2k_2} \end{pmatrix}, \quad j = 1,2 \tag{4.5}$$

where

$$\frac{\partial^2\omega_{1,2}(\vec{k},p)}{\partial^2 k_1} = \pm p\frac{\cos k_1(1-(p\cos k_1+q\cos k_2)^2)-p\sin^2 k_1(p\cos k_1+q\cos k_2)}{[(1-(p\cos k_1+q\cos k_2))(1+p\cos k_1+q\cos k_2)]^{3/2}}$$

$$\frac{\partial^2\omega_{1,2}(\vec{k},p)}{\partial^2 k_2} = \pm q\frac{\cos k_2(1-(p\cos k_1+q\cos k_2)^2)-q\sin^2 k_2(p\cos k_1+q\cos k_2)}{[(1-(p\cos k_1+q\cos k_2))(1+p\cos k_1+q\cos k_2)]^{3/2}}$$

$$\frac{\partial^2\omega_{1,2}(\vec{k},p)}{\partial k_1\partial k_2} = \mp pq\frac{(p\cos k_1+q\cos k_2)\sin k_1\sin k_2}{[(1-(p\cos k_1+q\cos k_2))(1+p\cos k_1+q\cos k_2)]^{3/2}}. \tag{4.6}$$

Thus we solve

$$\det H(\omega_j(\vec{k},p)) = 0, \tag{4.7}$$

where

$$\det H(\omega_{1,2}(\vec{k},p)) = -p^2(1-p)^2\frac{(\cos k_1+\cos k_2)^2}{(-1+p\cos k_1+q\cos k_2)^2(1+p\cos k_1+q\cos k_2)^2}. \tag{4.8}$$

It is not surprising that the equation (4.7) has the same solutions as the equation (3.16) for the original Grover walk. It is satisfied for $\vec{k}_0$, where

$$\cos k_1 = \cos k_2, \quad i.e.\ \vec{k}_0 = (k_1, \pm k_1) \tag{4.9}$$

for which the Hessian matrix is of rank one. The solution (4.9) for the singular but non-zero Hessian matrix leads to the velocities of the highest probability peaks that are

$$\vec{v}^{HP_p} = (v_1^{HP_p}, v_1^{HP_p}) = \left(\frac{d\omega_j}{dk_1}(\vec{k}_0,p), \frac{d\omega_j}{dk_2}(\vec{k}_0,p)\right), \quad j=1,2 \tag{4.10}$$

where $\vec{k}_0$ is given by (4.9). It leads, except for the central peak, to additional four peaks with velocities equal to the parameters of the generalized Grover walk

$$\begin{aligned}
\vec{v}_1^{HP_p} &= (\ \ p, \ \ q),\\
\vec{v}_2^{HP_p} &= (-p, \ \ q),\\
\vec{v}_3^{HP_p} &= (-p, -q),\\
\vec{v}_4^{HP_p} &= (\ \ p, -q).
\end{aligned} \tag{4.11}$$

The generalized Grover walk behave according to its parameter, the velocities of the probability peaks are determined by p. The probability distribution of the walk spreads as an ellipse with the equation

$$\frac{v_1^2}{p} + \frac{v_2^2}{q} \leq 1, \quad q = 1 - p. \tag{4.12}$$

Parameters $\sqrt{p}$ and $\sqrt{q}$ respond to the major and the minor semiaxes. The probability distribution is illustrated in Fig. (4.1) for the number of steps $t = 50$ and three different choices of the parameter p. It exhibits the localization effect of the walk. Parameters p and q are chosen from the interval $(0, 1)$. Nevertheless, Fig. (4.2) shows, what happens with the walk if $p = 1$ ($q = 0$). As we can see, the walk lost its interesting interference properties. After t steps its location is either at the origin or t steps on the left or t steps on the right from the origin. This three possibilities occur with the same probability $\frac{1}{3}$.

4.2 Decrease of the highest probability peaks

As for the the original Grover walk we are interested in the decrease of the highest probability peaks depending on the number of steps t. Our expectation is that this generalized type of walk has the same decline as the original Grover walk. Indeed, we found the continuous curve of stationary points of the phase appearing in the inverse Fourier transformation $\tilde{\omega}_j(k_1, k_2, p) = \omega_j(k_1, k_2, p) - \frac{\vec{m} \cdot \vec{k}}{t}$ which is given by $k_1 = \pm k_2$. This is the same result as for the original Grover walk. Also the highest probability peaks drop with the total number of steps t as its inverse value t^{-1}.

Fig. (4.3) we can see the numerical simulation of the dropping peaks for the generalized type of walk in comparison with the inverse value of the total number of steps t^{-1}. Moreover, in Fig. (4.4) the existence of the continuous curve of the stationary points is illustrated. Comparing Fig. (3.2) and (4.3) we see that the same initial state for the Grover and the generalized Grover walk gives only small differences. For certain number of steps (every third), the generalized type of walk has its very highest peak the central one, instead of the peaks at the border. With the increase of the total number of steps, starting at some critical number of steps t_0, the central peak becomes the most significant. If we omit the localizing peak, the same figure as for the Grover walk (3.2) is obtained. Note that the initial state is for the Grover walk was non-localizing.

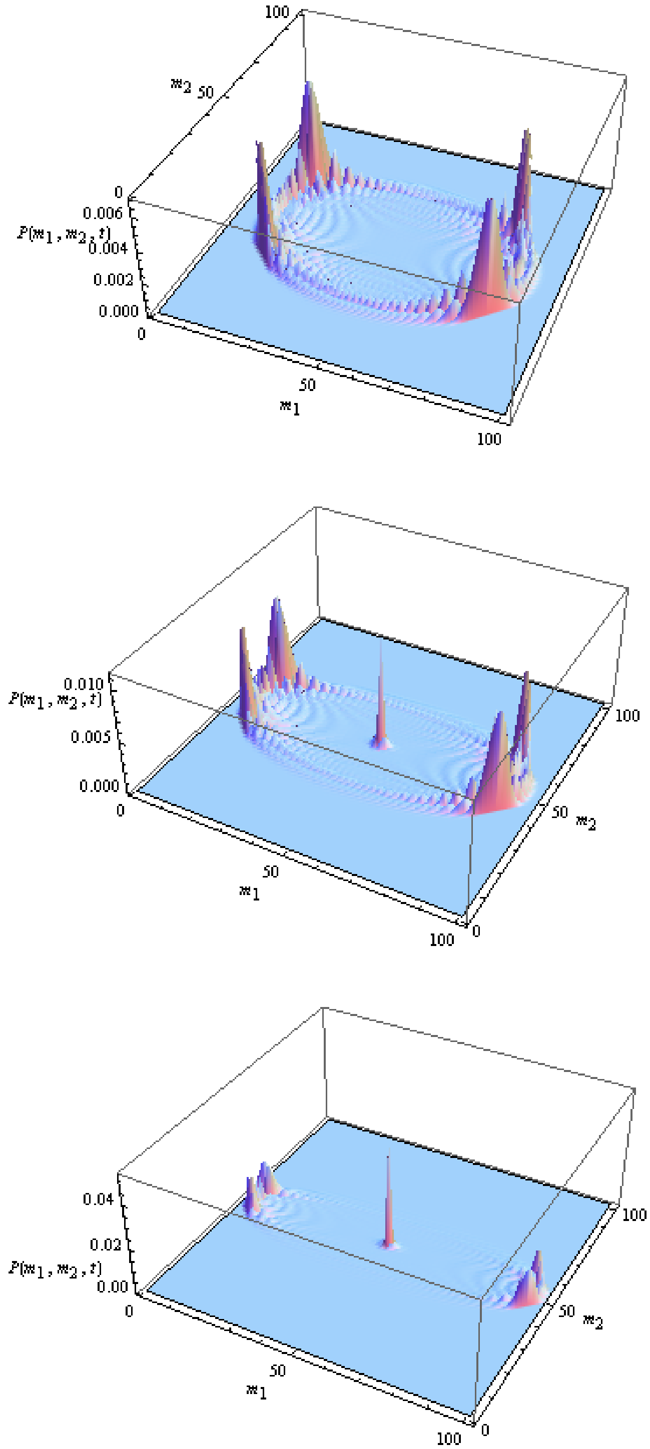

Figure 4.1: The probability distribution for the generalized Grover walk with coin (4.1) after number of steps $t = 50$. All plots are for the same initial state $\psi_0 \sim (\sqrt{2}, \sqrt{2}, 2, 2)$ and the parameter is for the first figure $p = \frac{2}{3}$, for the second $p = \frac{4}{5}$ and for the third $p = \frac{9}{10}$.

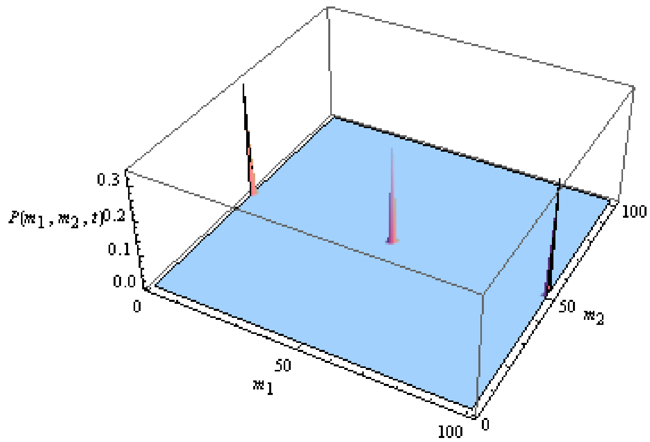

Figure 4.2: The probability distribution for the generalized Grover walk with coin (4.1) after $t = 50$ steps, the optional parameter is chosen $p = 1$.

4.3 Change of the basis variables

Consider the one-parameter family of coins with parameter p. As for the Grover walk we have two velocities for each direction $v_{1,2}^{(\pm)_p}$ that differ only in sign. Thus we can take for instance only $v_{1,2}^{(+)_p}$ and denote it as $v_{1,2}$. From the equations (4.4) we obtain for the moments $k_{1,2}$

$$\begin{aligned}
\sin k_1 &= \frac{2v_1\sqrt{pq - qv_1^2 - pv_2^2)}}{p\sqrt{(v_1+v_2+1)(v_1-v_2+1)(v_1+v_2-1)(v_1-v_2-1)}},\\
\cos k_1 &= \frac{(1+q)v_1^2 + pv_2^2 - p}{p\sqrt{(v_1+v_2+1)(v_1-v_2+1)(v_1+v_2-1)(v_1-v_2-1)}},\\
\sin k_2 &= \frac{2v_2\sqrt{pq - qv_1^2 - pv_2^2)}}{q\sqrt{(v_1+v_2+1)(v_1-v_2+1)(v_1+v_2-1)(v_1-v_2-1)}},\\
\cos k_2 &= -\frac{(1+p)v_2^2 + qv_2^2 - q}{q\sqrt{(v_1+v_2+1)(v_1-v_2+1)(v_1+v_2-1)(v_1-v_2-1)}},
\end{aligned} \tag{4.13}$$

where parameter $p \in (0,1)$ and $q = 1 - p$. Determinant of the Hessian matrix (4.5) is for frequencies $\omega_{1,2}(\vec{k}, p)$ from equation (4.3) given as

$$\det H(\omega_{1,2}(\vec{k}, p)) = -p^2(1-p)^2 \frac{(\cos k_1 + \cos k_2)^2}{(-1 + p\cos k_1 + q\cos k_2)^2(1 + p\cos k_1 + q\cos k_2)^2}.$$

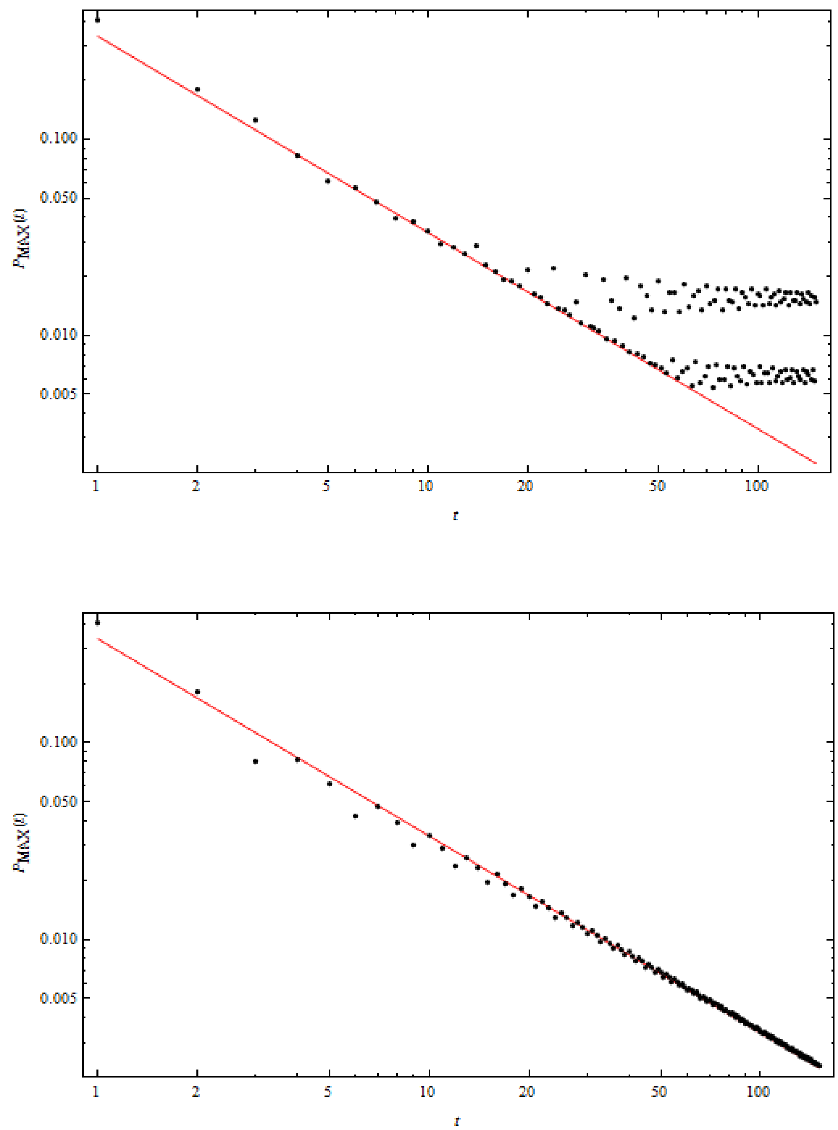

Figure 4.3: The decrease of the probability of the highest probability peaks with increasing total number of steps t. The probability value of the highest peaks (black points) is approximated by the red line $\sim t^{-1}$. Number of steps t ranges from 0 to 150 and both axes have logarithmic scale. The simulation is made for initial state $\psi_0 = \frac{1}{2}(1, 1, -1, -1)$ and the parameter of the walk is $p = \frac{1}{3}$ (i.e. $p = \frac{2}{3}$). In the top figure are distant points which illustrate the places where the central peak has overgrown the highest moving probability peaks. In the second graph is the central peak omitted.

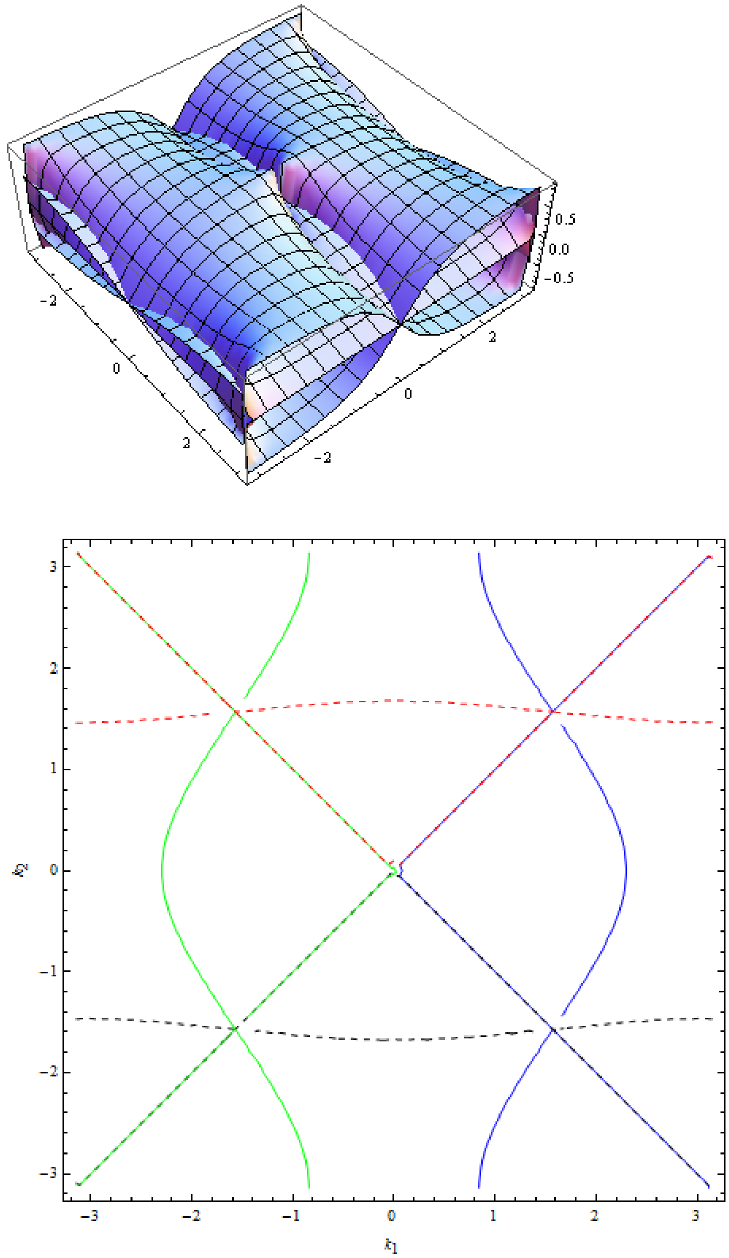

Figure 4.4: This figure represents contours of the velocities of the highest probability peaks for the generalized Grover walk with coin (4.1). The parameter p of the walk is $p = \frac{1}{5}$, it means $q = 1 - p = \frac{4}{5}$. The velocities for this type of walk are equal to $v_1^{HP_p} = \pm p$, $v_2^{HP_p} = \pm q$. Top figure illustrates the velocities $v_{1,2}^{(\pm)_p}$ from the equation (4.4). Blue and green lines in the bottom figure correspond to the contours where $v_1^{(\pm)_p} = \pm p$, red and black dashed line corresponds to the $v_2^{(\pm)_p} = \pm q$. The curve of stationary points is formed by $k_1 = \pm k_2$ and illustrated by mixing solid lines with dashed lines.

The results here are similar as for the Grover walk. In the velocity variables the determinant has the same form as for the Grover walk, also the Hessian matrix is singular for the same case. It is

$$\det H(\omega_{1,2}) = -\frac{1}{4}(v_1 + v_2 + 1)(v_1 - v_2 + 1)(v_1 + v_2 - 1)(v_1 - v_2 - 1) \quad (4.14)$$

is equal to zero if

$$\begin{aligned} |v1 + v_2| &= 1, \\ |v1 - v_2| &= 1. \end{aligned} \quad (4.15)$$

As we can see in the Fig. (4.3), considering that the velocities form the ellipse $\frac{v_1^2}{p} + \frac{v_2^2}{q} \leq 1$ with the interior points, the equations (4.15) are satisfied only for the highest peaks where

$$v_1 = \pm p, \quad v_2 = \pm q. \quad (4.16)$$

For the smaller peaks, located on the boundary of the ellipse, is the situation the same as for the Grover walk. The elements of the Hessian matrix, the second partial derivatives of the frequencies with respect to the wavenumbers $k_{1,2}$ are still on the boundary of the ellipse not defined. For instance

$$\frac{\partial^2 \omega_{1,2}}{\partial k_1^2} = \frac{p(1 + v_2^2) + v_1^2(2 - q - v_1^2 + v_2^2)}{2\sqrt{pq}\sqrt{1 - \frac{v_1^2}{p} - \frac{v_2^2}{q}}}. \quad (4.17)$$

Also from the Hessian matrix we cannot find the velocities of the smaller peaks located on the boundary of the ellipse, since the second derivatives are there not defined.

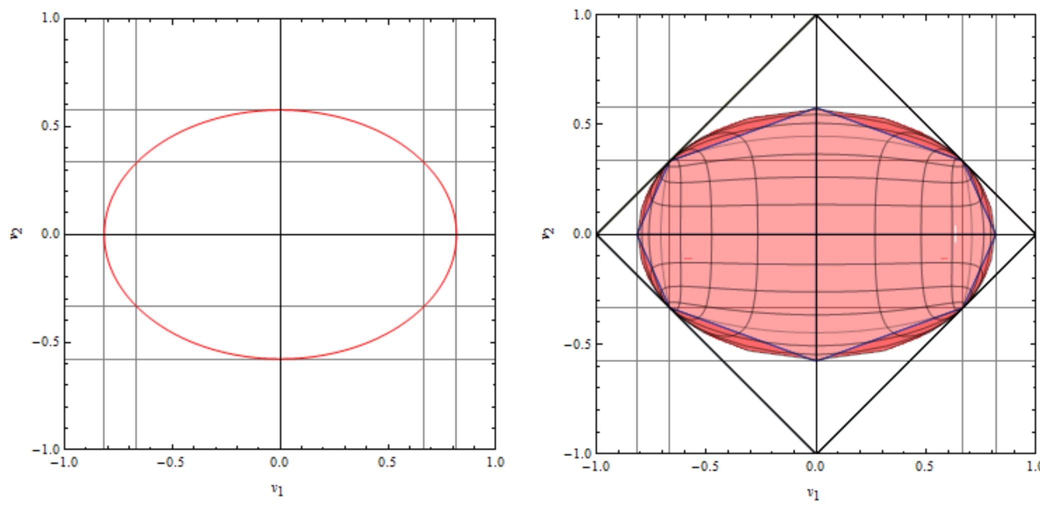

Figure 4.5: Parametric figure of the velocities $v_{1,2}^{(\pm)_p}$ from equation (4.4) on the right by red. The thick black lines correspond to the velocities corresponding to the singular Hessian matrix (equation (4.15)). The choice of the parameter p is $p = \frac{2}{3}$ i.e. $q = \frac{1}{3}$. The grid lines are in the horizontal direction on the positions $\pm p$ and $\pm\sqrt{p}$, in the vertical direction on the positions $\pm q$ and $\pm\sqrt{q}$. Lines $\pm\sqrt{p}, \pm\sqrt{q}$ correspond to the maximal velocity in appropriate direction, lines $\pm p, \pm q$ to the velocities of the highest peaks. The thick black lines touch the red region in the points belonging to the velocities of the highest probability peaks. The left figure illustrates the boundary of the red region on the right. The grid lines have the same positions.

Chapter 5

Generalized Grover walk on a square lattice with phase c

The second generalization of the two-dimensional Grover walk can by done using the same procedure as in the chapter 2. We would like to make continuous shift from the Grover coin G_4 to some permutation matrix. In the 4×4 case we have more possibilities what permutation matrix to choose. However, not every option is suitable.

Permutation matrix as the coin operator changes in each step the basis state of the coin space H_C. The walk takes place on the square network and we can present it as the composition of two one-dimensional walks on the line. Horizontal walk has as the basis of the coin space vectors $|L\rangle, |R\rangle$, the basis of the coin space for the walk on the vertical line is then given by vectors $|D\rangle, |U\rangle$. Thus there is no point in using such a permutation matrix which changes the basic states of the coin space between these two walks on the line. Using this argument these types of permutation matrices

$$P_1 = \begin{pmatrix} 0 & 0 & 0 & 1 \\ 0 & 0 & 1 & 0 \\ 0 & 1 & 0 & 0 \\ 1 & 0 & 0 & 0 \end{pmatrix}, \qquad \begin{array}{l} | L\rangle \longleftrightarrow | U\rangle \\ | R\rangle \longleftrightarrow | D\rangle \end{array}$$

$$P_2 = \begin{pmatrix} 0 & 0 & 1 & 0 \\ 0 & 0 & 0 & 1 \\ 1 & 0 & 0 & 0 \\ 0 & 1 & 0 & 0 \end{pmatrix}, \qquad \begin{array}{l} |L\rangle \longleftrightarrow |D\rangle \\ |R\rangle \longleftrightarrow |U\rangle \end{array}$$

can be excluded. The only important permutation matrix is such which changes the basic states only on the corresponding lines and does not switch between the horizontal and the vertical line. It is

$$\begin{aligned} |L\rangle &\longleftrightarrow |R\rangle \\ |U\rangle &\longleftrightarrow |D\rangle \end{aligned} \tag{5.1}$$

and the permutation matrix has form

$$P = \begin{pmatrix} 0 & 1 & 0 & 0 \\ 1 & 0 & 0 & 0 \\ 0 & 0 & 0 & 1 \\ 0 & 0 & 1 & 0 \end{pmatrix}. \tag{5.2}$$

As might be seen, there exist other permutation matrices that do not mix the basis state of the walk on the horizontal or the vertical lines. Those are such that switch in each step the basis vector only on one line and on the other line acts as identity

$$\begin{aligned} P_3 &= \begin{pmatrix} 0 & 1 & 0 & 0 \\ 1 & 0 & 0 & 0 \\ 0 & 0 & 1 & 0 \\ 0 & 0 & 0 & 1 \end{pmatrix}, \quad | L\rangle \longleftrightarrow | R\rangle \\ P_4 &= \begin{pmatrix} 1 & 0 & 0 & 0 \\ 0 & 1 & 0 & 0 \\ 0 & 0 & 0 & 1 \\ 0 & 0 & 1 & 0 \end{pmatrix}, \quad |D\rangle \longleftrightarrow |U\rangle. \end{aligned}$$

Nevertheless, as we will show at the end of the section, permutation matrices $P_{3,4}$ are also not appropriate choices.

We would like to find a matrix dependent on some continuous parameter that passes between the Grover and the permutation matrix

$$G_4 = \frac{1}{2}\begin{pmatrix} -1 & 1 & 1 & 1 \\ 1 & -1 & 1 & 1 \\ 1 & 1 & -1 & 1 \\ 1 & 1 & 1 & -1 \end{pmatrix} \longleftrightarrow P = \begin{pmatrix} 0 & 1 & 0 & 0 \\ 1 & 0 & 0 & 0 \\ 0 & 0 & 0 & 1 \\ 0 & 0 & 1 & 0 \end{pmatrix}.$$

Because any permutation of the basis states does not change the Grover matrix, we can find the shared eigenvalues of the Grover and the permutation matrix.

Nevertheless, the eigenvalues of our matrices are not the same, they differ in one eigenvalue. Knowledge of this and the spectral decomposition give us the one-parameter family of coins dependent on the continuous parameter.

To find a one-parameter family of coins dependent on some continuous parameter $c \in (0, \pi)$, which converts the Grover matrix G_4 to the permutation matrix P, we have to determine the shared eigenvectors from G_4 and P. Those are

$$\begin{aligned} v_1^{G_4,P} &= \frac{1}{2}(1,1,-1,-1)^T, \\ v_2^{G_4,P} &= \frac{1}{\sqrt{2}}(0,0,1,-1)^T, \\ v_3^{G_4,P} &= \frac{1}{\sqrt{2}}(1,-1,0,0)^T, \\ v_4^{G_4,P} &= \frac{1}{2}(1,1,1,1)^T. \end{aligned} \tag{5.3}$$

The corresponding eigenvalues for the permutation matrix P and the Grover matrix G_4 are

$$\begin{array}{llll} P: & \lambda_1^P = 1 & G_4: & \lambda_1^{G_4} = -1 \\ & \lambda_2^P = -1 & & \lambda_2^{G_4} = -1 \\ & \lambda_3^P = -1 & & \lambda_3^{G_4} = -1 \\ & \lambda_4^P = 1 & & \lambda_4^{G_4} = 1. \end{array} \tag{5.4}$$

Thus the Grover coin can be decomposed in the form

$$\begin{aligned} G_4 &= \textstyle\sum_{j=1}^4 \lambda_j^{G_4}(v_j^T \cdot v_j) \\ &= -v_1^T \cdot v_1 - v_2^T \cdot v_2 - v_3^T \cdot v_3 + v_4^T \cdot v_4 \end{aligned} \tag{5.5}$$

where we have marked $v_j = v_j^{G_4,P}, \;\; j \in \{1,2,3,4\}$.

The same eigenvectors $v_{2,3,4}$ correspond to the same eigenvalues $\lambda_{2,3,4}^{G_4,P}$. However the eigenvector v_1 belongs to different eigenvalues $\lambda_1^P = 1$ and $\lambda_1^{G_4} = -1$. It leads to the implementation of the phase factor e^{ic} in front of the first member of the sum (5.5). The resulting one-parameter family of coin has the form

$$\begin{aligned} G_4(c) &= -e^{ic}v_1^T \cdot v_1 - v_2^T \cdot v_2 - v_3^T \cdot v_3 + v_4^T \cdot v_4 \\ &= \frac{1}{4}\begin{pmatrix} -(1+e^{ic}) & 3-e^{ic} & 1+e^{ic} & 1+e^{ic} \\ 3-e^{ic} & -(1+e^{ic}) & 1+e^{ic} & 1+e^{ic} \\ 1+e^{ic} & 1+e^{ic} & -(1+e^{ic}) & 3-e^{ic} \\ 1+e^{ic} & 1+e^{ic} & 3-e^{ic} & -(1+e^{ic}) \end{pmatrix}. \end{aligned} \tag{5.6}$$

It will be shown that the one-parameter family of walks with coin $G_4(c)$ preserves the localization effect. The time evolution operator for the family of walks is

$$\tilde{U}(\vec{k},c) = \begin{pmatrix} e^{-ik_1} & 0 & 0 & 0 \\ 0 & e^{ik_1} & 0 & 0 \\ 0 & 0 & e^{-ik_2} & 0 \\ 0 & 0 & 0 & e^{ik_2} \end{pmatrix} \cdot G_4(c), \tag{5.7}$$

where $\vec{k} = (k_1, k_2)$. We are looking for the eigenvalues of the time evolution operator $\eta_j = e^{i\omega_j(\vec{k},c)}$, where $\omega_j(\vec{k},c)$ is the frequency. The eigenvalues are

$$\begin{aligned} \eta_{1,2} &= e^{i\omega_{1,2}(\vec{k},c)}, \\ \eta_{3,4} &= e^{i\omega_{3,4}(\vec{k},c)} = \pm 1. \end{aligned}$$

There are two constant eigenvalues having the same value as for the four-dimensional Grover time evolution operator (3.9). This indicates that the localization effect remained untouched.

We should note, why the permutation matrices $P_{3,4}$ are not appropriate choice. The Grover matrix has with these matrices the same shared eigenvectors as with the permutation matrix P, equation (5.3). However, the permutation matrices $P_{3,4}$ have two eigenvalues different. If we add phase factors in front of the two members in the spectral decomposition (5.5), we do not obtain a coin preserving the localization effect. Nevertheless, if we consider in the previous chapter as the parameter $p = 0$ or $p = 1$, the matrices $G(p)$ eq.(4.1) are equal to the permutation matrices P_3 or P_4. Thus we can say, that the previous case with parameter p includes remaining suitable permutation matrices.

5.1 Velocities of the probability peaks

The dependences of the frequencies $\omega_j(\vec{k},c)$ on the wave vector $\vec{k}$ correspond to the dispersion relations given by

$$\omega_{1,2}(\vec{k},c) = \frac{c}{2} \pm \arccos\left[-\frac{1}{2}(\cos k_1 + \cos k_2)\cos\frac{c}{2}\right]. \tag{5.8}$$

and

$$\omega_{3,4}(\vec{k},c) = 0. \tag{5.9}$$

The group velocities of the walk are given by the gradient of the frequencies $\omega_j,\ \ j \in \{1,2,3,4\}$ as follows:

$$\begin{aligned} \vec{v} &= \nabla_{\vec{k}}\omega_{1,2}(\vec{k},c) = (\frac{\partial\omega_{1,2}}{\partial k_1}(\vec{k},c), \frac{\partial\omega_{1,2}}{\partial k_2}(\vec{k},c)) \\ \vec{v}_S &= \nabla_{\vec{k}}\omega_{3,4}(\vec{k},c) = \vec{0}. \end{aligned} \tag{5.10}$$

The first equation from (5.10) results in

$$\begin{aligned} v_1^{(\pm)_{phase}} &= \pm\frac{\cos\frac{c}{2}\sin k_1}{\sqrt{(2-\cos\frac{c}{2}(\cos k_1+\cos k_2))(2+\cos\frac{c}{2}(\cos k_1+\cos k_2))}}, \\ v_2^{(\pm)_{phase}} &= \pm\frac{\cos\frac{c}{2}\sin k_2}{\sqrt{(2-\cos\frac{c}{2}(\cos k_1+\cos k_2))(2+\cos\frac{c}{2}(\cos k_1+\cos k_2))}}, \end{aligned} \tag{5.11}$$

where $\vec{v} = (v_1^{(\pm)_{phase}}, v_2^{(\pm)_{phase}})$.

As in the section (3.1) we are looking for the group velocity of the highest probability peaks. This velocity is found at the point $\vec{k} = \vec{k}_0$ where the Hessian matrix is singular. The group velocity $\vec{v}_S$ for $\omega_{3,4}$ is easily solved using equation (5.11) and belongs to the central locating peak. Thus we are interested only in $\omega_{1,2}(\vec{k},c)$. We have to solve when the Hessian matrix

$$H(\omega_j(\vec{k},c)) = \begin{pmatrix} \frac{d^2\omega_j(\vec{k},c)}{d^2k_1} & \frac{d^2\omega_j(\vec{k},c)}{dk_1dk_2} \\ \frac{d^2\omega_j(\vec{k},c)}{dk_2dk_1} & \frac{d^2\omega_j(\vec{k},c)}{d^2k_2} \end{pmatrix}, \quad j = 1,2 \tag{5.12}$$

has its determinant

$$\det H((\omega_j(\vec{k},c))) = \frac{2a^4\cos 2k_1 + 8a^2(a^2-2)\cos k_1\cos k_2 + 2a^4(2+\cos 2k_2)}{4(-2+a(\cos k_1+\cos k_2))^2(2+a(\cos k_1+\cos k_2))^2} \tag{5.13}$$

equal to zero. The second derivatives are

$$\begin{aligned} \frac{\partial^2\omega_{1,2}(\vec{k},c)}{\partial^2k_1} &= \pm a\frac{\cos k_1(4-a^2(\cos k_1+\cos k_2)^2) - a^2\sin^2 k_1(\cos k_1+\cos k_2)}{[(2-a(\cos k_1+\cos k_2))(2+a(\cos k_1+\cos k_2))]^{3/2}}, \\ \frac{\partial^2\omega_{1,2}(\vec{k},c)}{\partial^2k_2} &= \pm a\frac{\cos k_2(4-a^2(\cos k_1+\cos k_2)^2) - a^2\sin^2 k_2(\cos k_1+\cos k_2)}{[(2-a(\cos k_1+\cos k_2))(2+a(\cos k_1+\cos k_2))]^{3/2}}, \\ \frac{\partial^2\omega_{1,2}(\vec{k},c)}{\partial k_1\partial k_2} &= \pm a^3\frac{(\cos k_1+\cos k_2)\sin k_1\sin k_2}{[(2-a(\cos k_1+\cos k_2))(2+a(\cos k_1+\cos k_2))]^{3/2}}, \end{aligned} \tag{5.14}$$

where we have identified

$$a = \cos\frac{c}{2}. \tag{5.15}$$

Here we have to divide the solution according to the rank of the Hessian matrix. The highest probability peaks are now located at the position, where the Hessian matrix is the zero matrix. It is satisfied for

$$\vec{k}_0 = \left(\pm\frac{\pi}{2}, \pm\frac{\pi}{2}\right). \tag{5.16}$$

Now the equations (5.11) give us the velocities of the highest moving probability peaks

$$\vec{v}^{HP_{phase}} = (v_1^{HP_{phase}}, v_2^{HP_{phase}}) = \left(\frac{\partial\omega_{1,2}}{\partial k_1}(\vec{k}_0, c), \frac{\partial\omega_{1,2}}{\partial k_2}(\vec{k}_0, c)\right) \tag{5.17}$$

that are

$$\begin{aligned}
\vec{v}_1^{HP_{phase}} &= \left(\frac{1}{2}\cos\frac{c}{2}, \frac{1}{2}\cos\frac{c}{2}\right), \\
\vec{v}_1^{HP_{phase}} &= \left(-\frac{1}{2}\cos\frac{c}{2}, \frac{1}{2}\cos\frac{c}{2}\right), \\
\vec{v}_1^{HP_{phase}} &= \left(-\frac{1}{2}\cos\frac{c}{2}, -\frac{1}{2}\cos\frac{c}{2}\right), \\
\vec{v}_1^{HP_{phase}} &= \left(\frac{1}{2}\cos\frac{c}{2}, -\frac{1}{2}\cos\frac{c}{2}\right).
\end{aligned} \tag{5.18}$$

The vector $\vec{k}_0$ leads to the Hessian matrix with rank equal to zero. In the previous cases we found that the Hessian matrix is singular with rank equal to one for $k_1 = \pm k_2$ and it led to the velocities of the highest peaks. The Hessian matrix has rank equal to one for

$$\cos k_2 = \frac{2\cos k_1 - a^2\cos k_1 \pm 2\cos k_1\sqrt{1-a^2}}{a^2}, \tag{5.19}$$

provided that

$$a = \cos\frac{c}{2} \neq 0, \quad \Rightarrow \quad c \neq 0; \pi. \tag{5.20}$$

The phase $c = 0$ corresponds to the Grover walk and $c = \pi$ is the trivial walk with permutation matrix (5.2) as its coin. It is not necessary to consider both signs plus and minus in front of the square root in (5.19). The only difference is that the velocities $v_{1,2}^{(\pm)_{phase}}$ are shifted by π, but the norm

$v^{(\pm)_{phase}} = \sqrt{(v_1^{(\pm)_{phase}})^2 + (v_2^{(\pm)_{phase}})^2}$ remains unchanged. Further in the text we will consider only the solution (5.19) with minus sign.

The solution (5.19) does not lead to the same velocities as for the highest peaks. Thus it has to correspond to the smaller probability peaks. The equations (5.11, 5.19) imply for the velocities of the smaller peaks

$$\begin{aligned} v_1^{SP_{phase}} &= \pm\frac{a^2 \sin k_1}{2\sqrt{a^2+\cos^2 k_1(a^2-2+2\sqrt{1-a^2})}}, \\ v_2^{SP_{phase}} &= \pm\frac{1}{2}\sqrt{\frac{a^4-(\cos k_1(a^2-2+2\sqrt{1-a^2}))^2}{a^2+\cos^2 k_1(a^2-2+2\sqrt{1-a^2})}}, \end{aligned} \tag{5.21}$$

where

$$\vec{v}^{SP_{phase}} = (v_1^{SP_{phase}}, v_2^{SP_{phase}}). \tag{5.22}$$

The probability distribution of the walk is shown in the Fig. (5.1) for several phases c.We see that the boundary of the walk is formed by the probability peaks. The highest peaks appear in four symmetrically distributed locations. The rest of the boundary is formed by the smaller peaks. Further, the region covered by the walk decreases with the increasing phase c and the smaller peaks become more significant. For the trivial walk with phase $c = \pi$ the probability distribution is formed only by the central peak. In all figures is the initial state chosen such that the central peak disappears (except for the walk with phase $c = 0$). This initial state is the same as for the Grover walk $\psi_0 = \frac{1}{2}(1, 1, -1, -1)$. However for the one-parameter family of coins with parameter p and the initial state ψ_0 the central peak does not disappear for arbitrary choice of p. In addition, to obtain the probability distribution without the central peak, we need different initial state for each p.

In the figures (5.2) and (5.3) we see that the velocities $\vec{v}^{SP_{phase}}$ from equation (5.21) truly correspond to the boundary of the probability distribution, i.e. to the smaller probability peaks. For the phase $c \in (0, \pi)$ are there chosen two values $c = \frac{\pi}{2};\ \frac{\pi}{8}$. In the figures (5.1) and (5.1) are illustrated appropriate velocities of the smaller peaks $v_{1,2}^{SP_{phase}}$ in comparison with the velocities describing the walk $v_{1,2}^{(\pm)_{phase}}$ from equation (5.11). Each of these figures has four horizontal and four vertical grid lines depicting the velocities of the highest peaks and the maximal velocities in both directions. The velocities are complex in general, both real and

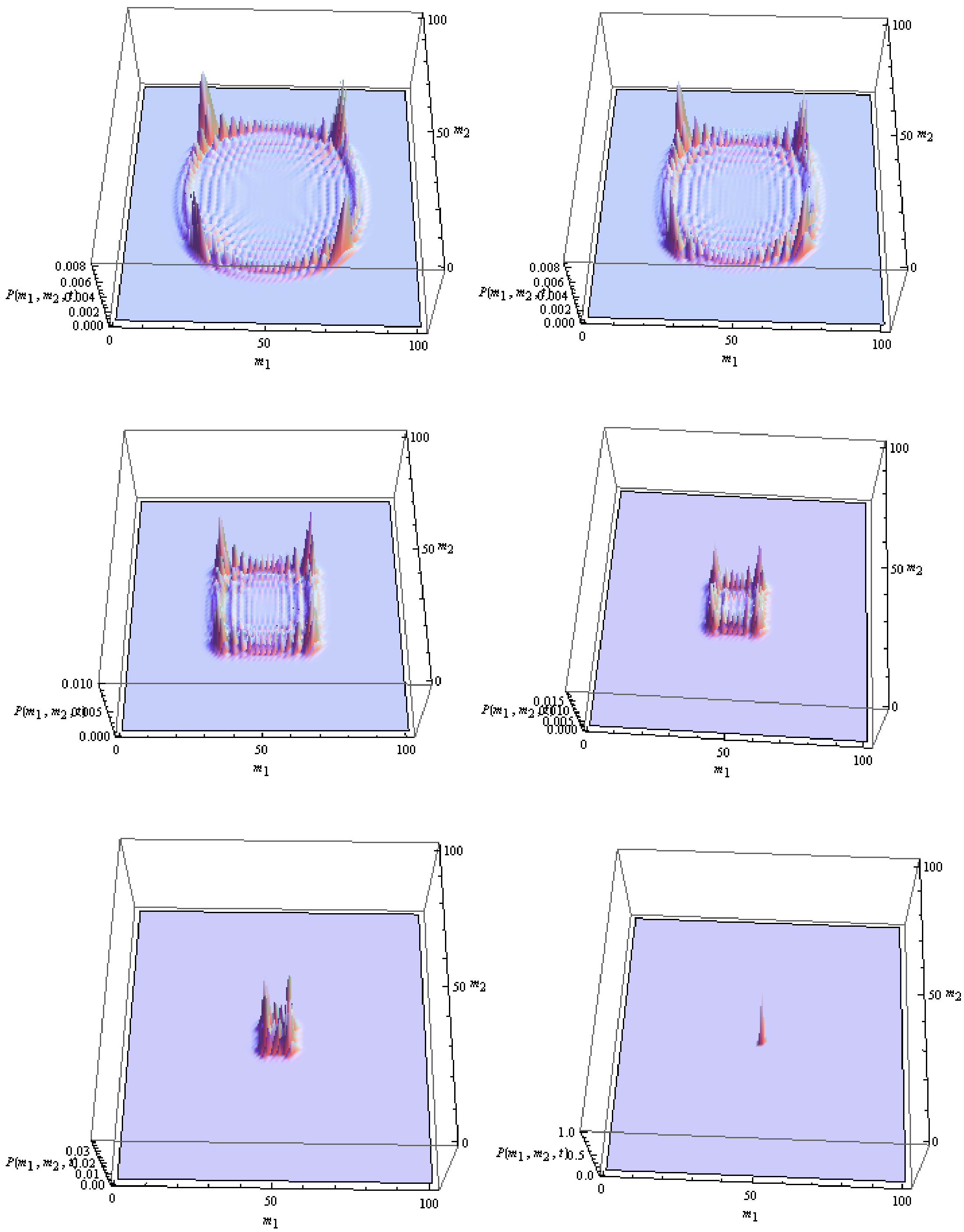

Figure 5.1: The probability distributions for the family of Grover walks with phase c. The number of steps is $t = 50$ and the initial state $\psi_0 = \frac{1}{2}(1, 1, -1, -1)$ is for all figures the same. The phases, starting from the figure in the upper left corner, are $c = \frac{\pi}{8}, \frac{\pi}{4}, \frac{\pi}{2}, \frac{3\pi}{4}, \frac{7\pi}{8}, \pi$.

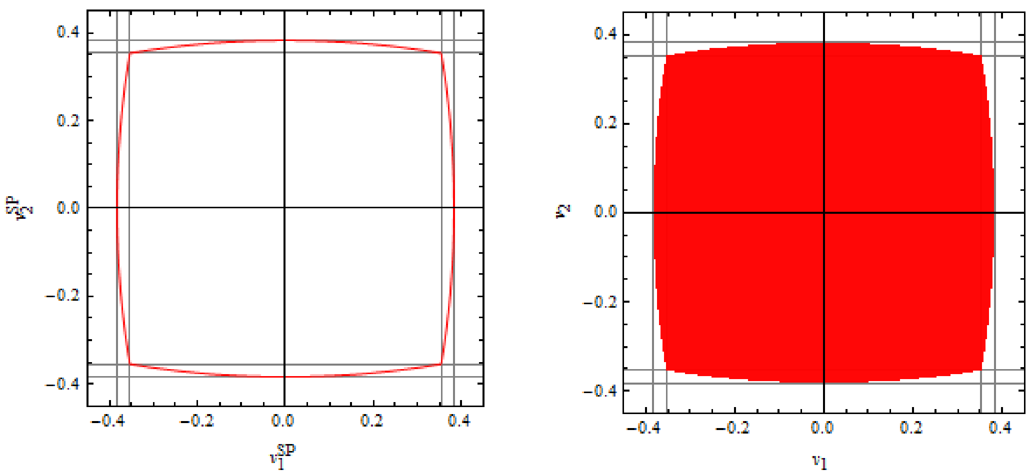

Figure 5.2: Parametric figures of the velocities $\vec{v}^{SP_{phase}} = ({v_1}^{SP_{phase}}, {v_2}^{SP_{phase}}) = (v_1^{SP}, v_2^{SP})$ from equation (5.21) on the left and $\vec{v}^{phase} = ({v_1}^{(\pm)_{phase}}, {v_2}^{(\pm)_{phase}}) = (v_1, v_2)$ from equation (5.11) on the right. The right figure illustrates the velocities of the walk by red. It also depict the shape of the region covered by the walk. The left figure corresponds to the velocities of the probability peaks (5.21), it forms a boarder of the velocities on the right figure. The phase of the walk is $c = \frac{\pi}{2}$. Grid lines represent important velocities. Outer lines correspond to the maximal velocities that are $v_{1,2} = v_{1,2}^{MAX} \doteq \pm 0,3827$. Inner lines correspond to the velocities of the highest probability peaks that are $v_{1,2} = v_{1,2}^{HP} = \frac{1}{2} \cos \frac{\pi}{4} \doteq \pm 0,3536$.

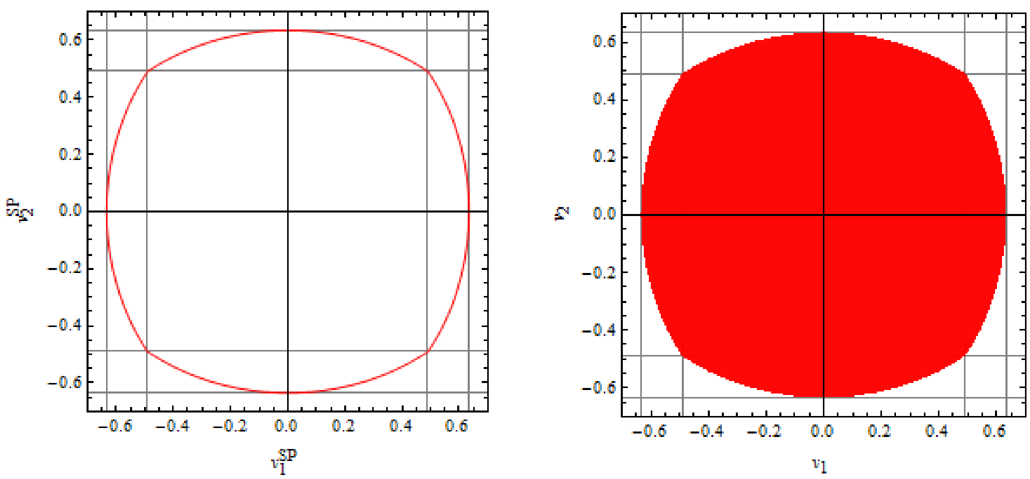

Figure 5.3: Parametric figures of the velocities $\vec{v}^{SP_{phase}} = ({v_1}^{SP_{phase}}, {v_2}^{SP_{phase}}) = (v_1^{SP}, v_2^{SP})$ from equation (5.21) on the left and $\vec{v}^{phase} = ({v_1}^{(\pm)_{phase}}, {v_2}^{(\pm)_{phase}}) = (v_1, v_2)$ from equation (5.11) on the right. The right figure illustrates the velocities of the walk by red and also depict the shape of the region covered by the walk. The left figure corresponds to the velocities of the probability peaks (5.21), it forms a boarder of the right plot. The phase of the walk is $c = \frac{\pi}{8}$. Grid lines represent important velocities. Outer lines correspond to the maximal velocities that are $v_{1,2} = v_{1,2}^{MAX} \doteq \pm 0,6344$. Inner lines correspond to the velocities of the highest probability peaks that are $v_{1,2} = v_{1,2}^{HP} = \frac{1}{2} \cos \frac{\pi}{16} \doteq \pm 0,4904$.

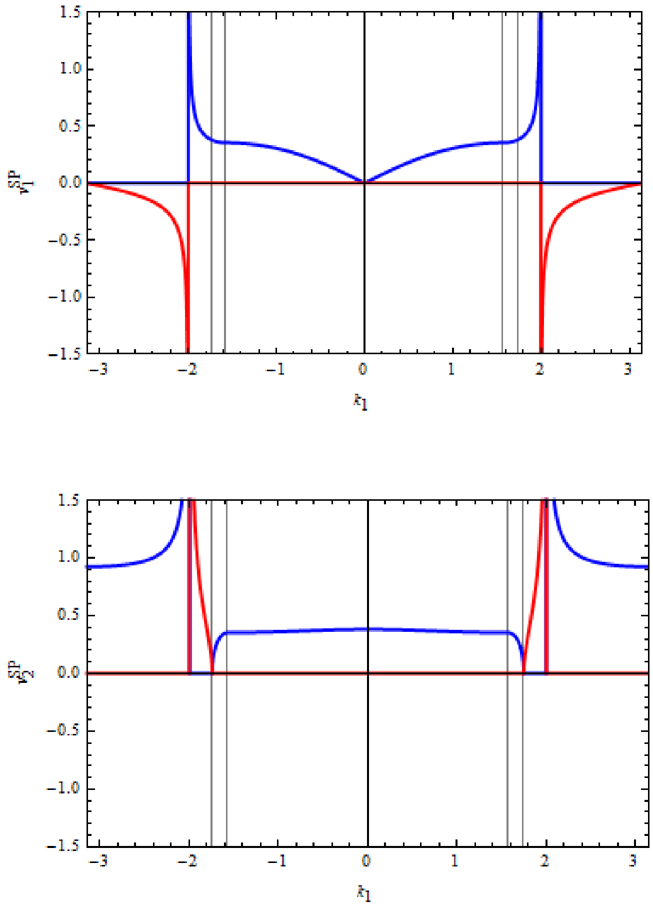

Figure 5.4: Figures of the positive velocities $v_{1,2}^{SP_{phase}} = v_{1,2}^{SP}$ from equation (5.21) for the phase $c = \frac{\pi}{2}$, i.e. $a = \cos\frac{\pi}{4}$. The velocities are complex in general. The real part is given by thick blue line, imaginary part is given by thick red line. Grid lines depict interesting velocities. Grid line for $k_1 = 0$ shows zero velocity in the horizontal direction, bud maximal velocity in the vertical direction. Outer grid lines depict the maximal velocity in the horizontal direction, but zero velocity in the vertical direction that arise for $k_1 = k_1^{MAX} \doteq \pm 1,7432$. Inner bud not central grid lines show the velocities of the maximal probability peaks, where the velocities on both horizontal and vertical lines are equal. It occurs for $k_1 = \pm\frac{\pi}{2}$.There is no point in taking momentum k_1 out of the range $(-k_1^{MAX}, k_1^{MAX})$ because out of it is always one of the velocities purely imaginary.

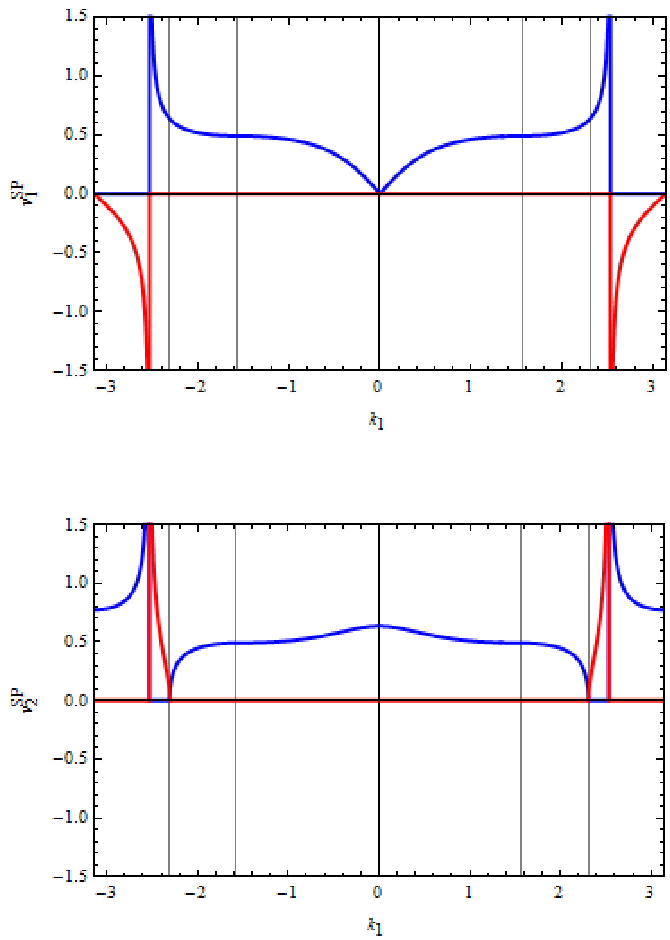

Figure 5.5: Figures of the positive velocities $v_{1,2}^{SP_{phase}} = v_{1,2}^{SP}$ from equation (5.21) for the phase $c = \frac{\pi}{8}$, i.e. $a = \cos\frac{\pi}{16}$. The velocities are complex in general. The real part is given by thick blue line, imaginary part is given by thick red line. Grid lines depict interesting velocities. Grid line for $k_1 = 0$ shows zero velocity in the horizontal direction, bud maximal velocity in the vertical direction. Outer grid lines depict the maximal velocity in the horizontal direction, but zero velocity in the vertical direction that arise for $k_1 = k_1^{MAX} \doteq \pm 2,3097$. Inner bud not central grid lines show the velocities of the maximal probability peaks, where the velocities on both horizontal and vertical lines are equal. It occurs for $k_1 = \pm\frac{\pi}{2}$. There is no point in taking momentum k_1 out of the range $(-k_1^{MAX}, k_1^{MAX})$ because out of it is always one of the velocities purely imaginary.

imaginary part are plotted. Maximal (minimal) velocities are given by

$$v_{1,2}^{MAX_{phase}} = \pm\sqrt{\frac{-2+2a^2+2\sqrt{1-a^2}-a^2\sqrt{1-a^2}}{-2+2a^2+a\sqrt{1-a^2}}}. \qquad (5.23)$$

Maximal velocity in the second direction $v_2^{SP_{phase}} = v_2^{MAX_{phase}}$ appears always for $k_1 = 0$ and the velocity $v_1^{SP_{phase}}$ is at the same time equal to zero. This relationship is satisfied also conversely, i.e. if $v_1^{SP_{phase}} = v_1^{MAX_{phase}}$ than at the same time the velocity $v_1^{SP_{phase}} = 0$. It seems not to be possible to find unique explicit solution for k_1 where the velocity $v_1^{SP_{phase}} = v_1^{MAX_{phase}}$ together with the velocity $v_2^{SP_{phase}} = 0$. It is because the velocities are in general complex. Nevertheless, it is easy to enumerate for some c appropriate value of k_1 where $v_2^{SP_{phase}} = 0$ if we know the value of the phase c of the walk. From the velocities of the smaller peaks we can simply obtain the velocities of the highest peaks. There are several ways how to do that. The highest peaks appear if $k_{1,2} = \pm\frac{\pi}{2}$. Let $k_1 = \pm\frac{\pi}{2}$, then from equation (5.19) we get $k_2 = \pm\frac{\pi}{2}$. Also

$$v_{1,2}^{SP_{phase}}|_{k_1=\pm\frac{\pi}{2}} = v_{1,2}^{HP_{phase}}. \qquad (5.24)$$

Further we know that maximal peaks have absolute value of its velocities in both direction equal. Therefore solution of the equation $v_1^{SP_{phase}} = v_2^{SP_{phase}}$ give us the velocities of the highest peaks too. Moreover, as we might from the further computations assume,

$$\frac{dv_{1,2}^{SP_{phase}}}{dk_1}|_{\pm\frac{\pi}{2}} = 0. \qquad (5.25)$$

Thus the highest peaks of the walk are given by the stationary points of the velocities on the boundary.

5.2 Decrease of the highest probability peaks

It was shown that the decreasing behavior of the highest peaks has for the Grover walk and for the one-parameter family of Grover walks with parameter p the same character. They decrease proportional to the inverse value of the total number of steps. This behavior was explained using the theory of stationary phase. For the family of Grover walks with phase c the situation is different. In the figures (5.6),(5.7)we can see the decreasing value of the dominant probability peaks in dependence on the increasing number of steps. There is still a number of open questions in the theory of the asymptotic expansion of double integrals. We are interested in the vector of probability amplitudes given by the integral (3.10) dependent on the phase and its behavior for $t \to \infty$. It has the form

$$\psi(\vec{m}, c, t) = \frac{1}{(2\pi)^2} \sum_{j=1}^{4} \int_{-\pi}^{\pi} dk_1 \int_{-\pi}^{\pi} dk_2 e^{i(\omega_j(\vec{k},c) - \frac{\vec{m}\cdot\vec{k}}{t})t} (v_j(\vec{k}, c), \psi_0) v_j(\vec{k}, c), \quad (5.26)$$

where $j \in \{1, 2, 3, 4\}$. The expansion of this type of integral can be found in [3], where the results are divided according to the properties of the integral. However none of the results coincides with the numerical results seen in the figures (5.6),(5.7). The highest probability peaks of the walk for phases $c \geq \frac{\pi}{2}$ (figure (5.6)) decreases as $t^{-\frac{6}{5}}$, where t is the total number of steps. The simulation is made for t ranges from 0 to 150. The deviations of the maximal probabilities from the power law approximation is slightly greater than it was for the Grover walk and the walk with parameter p. However for increasing number of steps the deviations are still less significant. The probability of finding the particle at position $\vec{m}$ in time t is square of norm of the probability amplitudes vector. Thus $\psi(\vec{m}^{HP}, c, t) \sim t^{-\frac{3}{5}}$, where $\vec{m}^{HP}$ is the location of the highest probability peaks.

For the phases $c < \frac{\pi}{2}$ is the situation illustrated in the figure (5.7). The decrease in the logarithmic scale is not entirely linear as before. The highest peaks correspond to the zero Hessian matrix, nevertheless all expansions of our type of integrals are solved for non-zero Hessian matrix.

5.3 Change of the basis variables

One can see that the previous Grover walk and the generalized Grover walk with parameter p have many similar features. In addition, in this chapter we have seen, that the generalized Grover walk with phase c behaves slightly different. Here the behavior is also different. We can switch from the wavenumbers $k_{1,2}$ using the equations (5.11) into the velocity variables $v_{1,2}^{(+)_{phase}}$, but the resulting

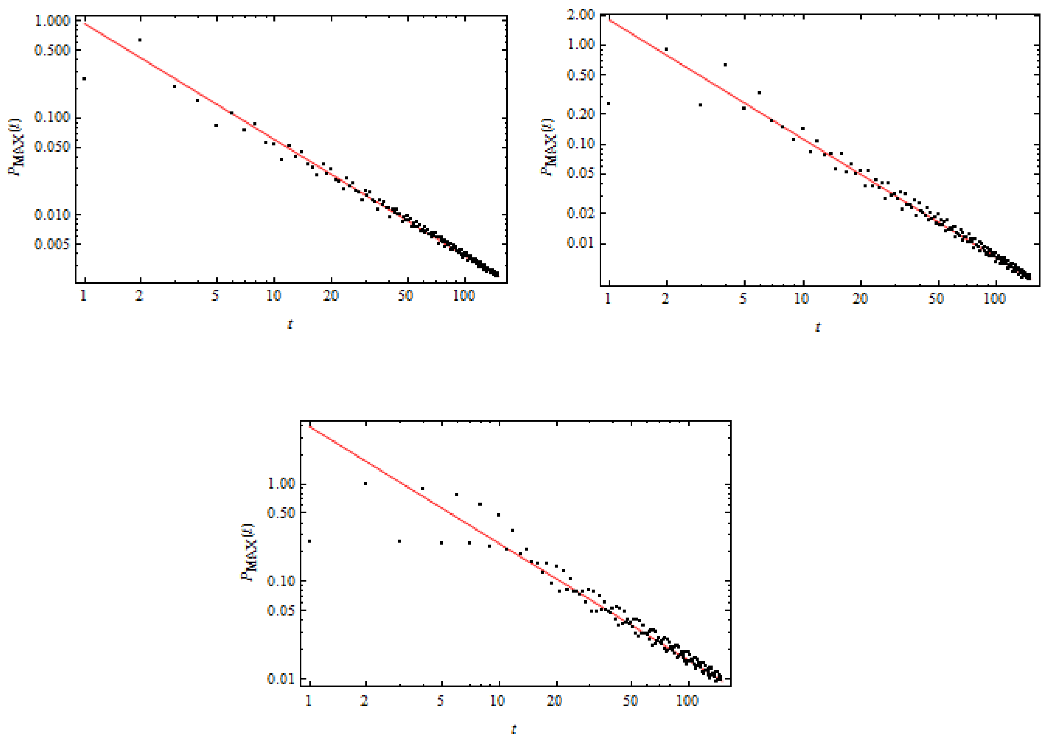

Figure 5.6: The decrease of the maximal probability peaks in dependence on the number of steps t. For better recognition the logarithmic scale on both axes is used. Black points correspond to the probability value of the highest peaks and the red line is the approximation $t^{\frac{6}{5}}$. The figures are made for three different choices of the phases $c = \frac{\pi}{2}, \frac{3\pi}{4}, 7\pi 8$ starting from the figure in the upper left corner. The initial state for the walk is $\psi_0 = \frac{1}{2}(1, 1, -1, -1)$.

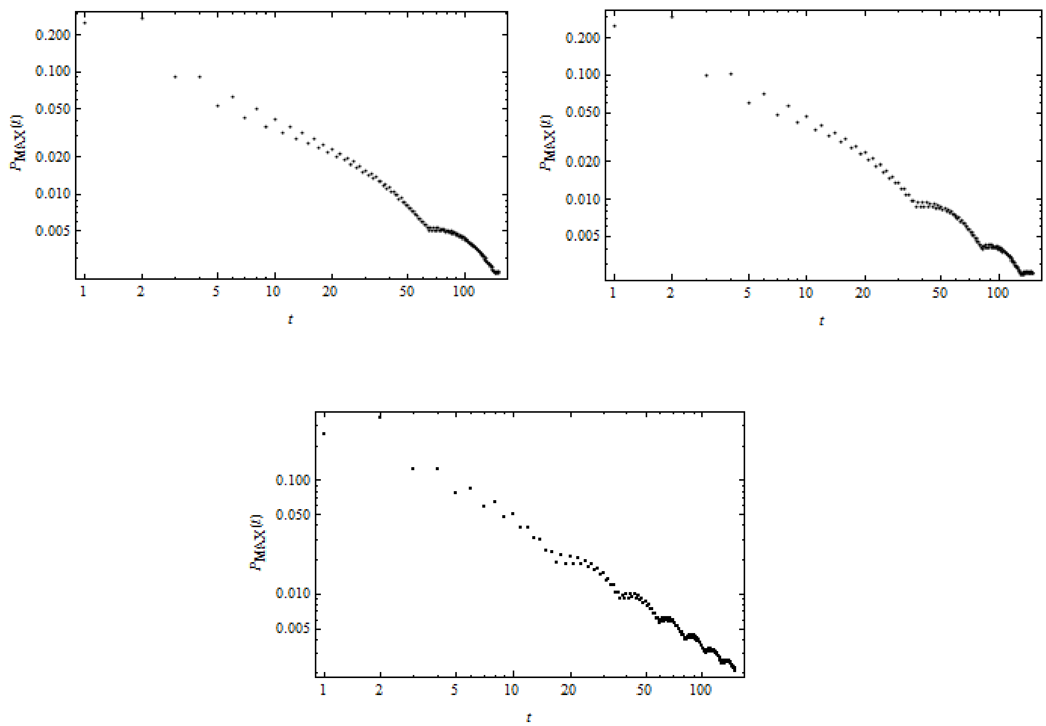

Figure 5.7: The decrease of the maximal probability peaks in dependence on the number of total steps t. The logarithmic scale on both axes was used. Black points correspond to the probability value of the highest peaks. The figures are made for three different choices for the phase. It is $c = \frac{\pi}{8}, \frac{\pi}{6}, \pi 4$ starting from the figure in the upper left corner. The initial state for the walk is $\psi_0 = \frac{1}{2}(1, 1, -1, -1)$. We see that due to the behavior of the highest peaks the approximation t^{-x} does not fit very well for any x.

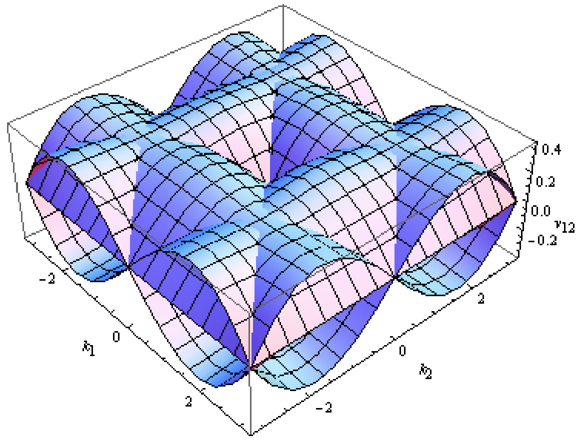

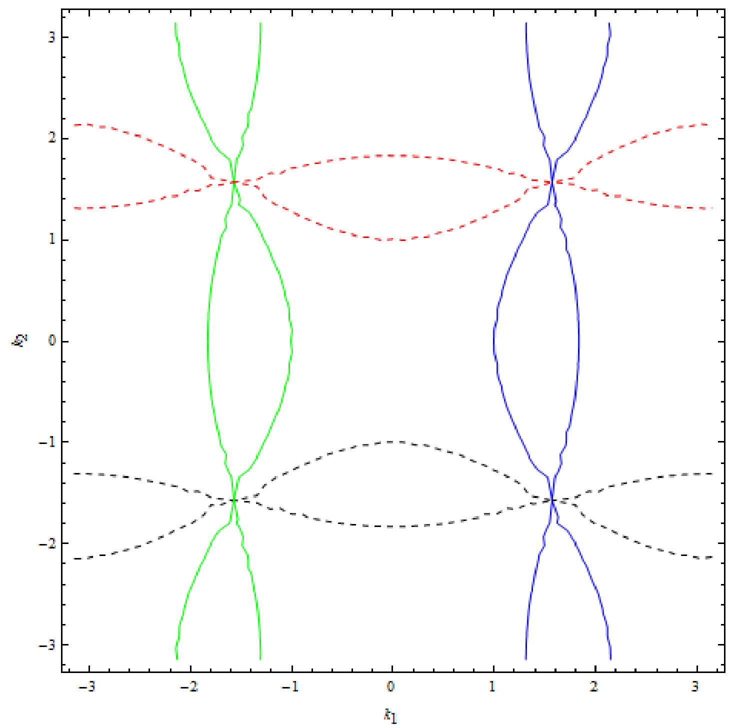

Figure 5.8: Figure representing contours of the velocities of the highest probability peaks for the one-parameter family of walks with phase c. This figure is made for the parameter $c = \frac{\pi}{2}$ i.e. $a = \cos\frac{\pi}{4} = \frac{1}{\sqrt{2}}$. The velocities represented by the contours are $v_{1,2}^{(\pm)_{phase}} = v_{1,2}^{HP}$ from equations (5.18). Blue and green lines correspond to the $v_1^{(\pm)_{phase}} = \frac{1}{2}a$, red and black dashed lines corresponds to the $v_2^{(\pm)_{phase}} = \frac{1}{2}a$, where $a = \cos\frac{c}{2}$. It is seen that there is no curve of stationary points as in the Grover case and the generalized Grover case with parameter p (Fig. (3.3, 4.4)). First figure illustrates the velocities $v_{1,2}^{(\pm)_{phase}}$.

relations are much more difficult. The equations are

$$
\begin{aligned}
\sin k_1 &= \frac{v_1}{a}\sqrt{\frac{-2(a^2+2(-1+v_1^2+v_2^2))-2f(v_1,v_2,a)}{(v_1+v_2+1)(v_1-v_2+1)(v_1+v_2-1)(v_1-v_2-1)}}\\
\cos k_1 &= \frac{1}{a}\sqrt{\frac{4v_1^2(-1+v_1^2+v_2^2)+a^2(1+v_1^4+v_2^4-2(1+v_1^2)v_2^2)+2v_1^2f(v_1,v_2,a)}{(v_1+v_2+1)(v_1-v_2+1)(v_1+v_2-1)(v_1-v_2-1)}}\\
\sin k_2 &= \frac{v_2}{a}\sqrt{\frac{-2(a^2+2(-1+v_1^2+v_2^2))-2f(v_1,v_2,a)}{(v_1+v_2+1)(v_1-v_2+1)(v_1+v_2-1)(v_1-v_2-1)}}\\
\cos k_2 &= -\frac{1}{a}\sqrt{\frac{4v_2^2(-1+v_1^2+v_2^2)+a^2(1+v_1^4+v_2^4-2(1+v_2^2)v_1^2)+2v_2^2f(v_1,v_2,a)}{(v_1+v_2+1)(v_1-v_2+1)(v_1+v_2-1)(v_1-v_2-1)}}
\end{aligned}
\tag{5.27}
$$

where we denoted $v_{1,2}^{(+)_{phase}} = v_{1,2}$, $a = \cos\frac{c}{2}$ and

$$f(v_1,v_2,a) = \sqrt{a^4+16v_1^2v_2^2+4a^2(v_1^4+v_2^4-v_2^2-v_1^2(1+2v_2^2))}. \tag{5.28}$$

The determinant of the Hessian matrix $H(\omega_j(\vec{k},c))$, where $\omega_j(\vec{k},c)$ are given in equation (5.8), is in the momentum variables

$$\det H((\omega_j(\vec{k},c))) = \frac{2a^4\cos 2k_1 + 8a^2(a^2-2)\cos k_1\cos k_2 + 2a^4(2+\cos 2k_2)}{4(-2+a(\cos k_1+\cos k_2))^2(2+a(\cos k_1+\cos k_2))^2}.$$

Switching of the determinant into the velocity variables does not bring a great simplification. Thus we do not specify here the expression for its complexity, nevertheless we present the result graphicaly.

In figure (5.3) the determinant of the Hessian matrix depending on the velocities $v_{1,2}$ is given. As we can see, for certain velocities are in the figure empty places. It indicates that the determinant is for those velocities not real. The only part of the determinant which can acquire imaginary values is one square root that is equal to the function f from equation (5.28). The function is depicted in figure (5.10). Indeed, comparing the figures (5.3) and (5.10) we see that the function f is responsible for the imaginary value of $\det H$. Moreover, it can be seen that the central parts of the figures noticeably remind the regions covered by the walk, i.e. the velocities of the walk depicted in the figures (5.1, 5.2, 5.3). Further we might be interested if there exist simple solution for the region, where the function f becomes imaginary. Solving the equation

$$f(v_1,v_2,a) = 0 \tag{5.29}$$

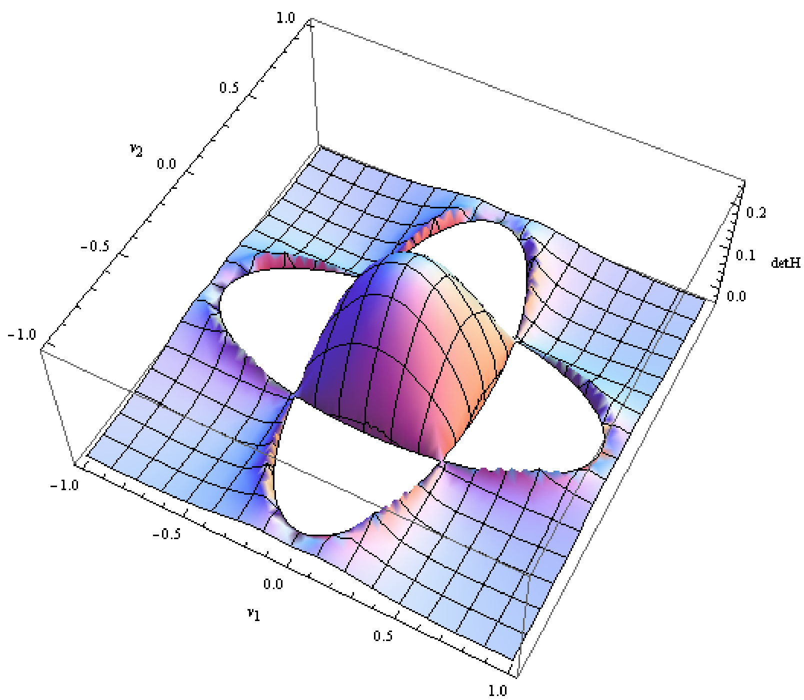

Figure 5.9: Figure illustrating the determinant of the Hessian matrix in the velocity variables for the family of Grover walks with phase c. The choice for the phase is $c = \frac{\pi}{2}$, i.e. $a = \cos\frac{c}{2} = \frac{1}{\sqrt{2}}$. The formula for the determinant is for its complexity not given in the text.

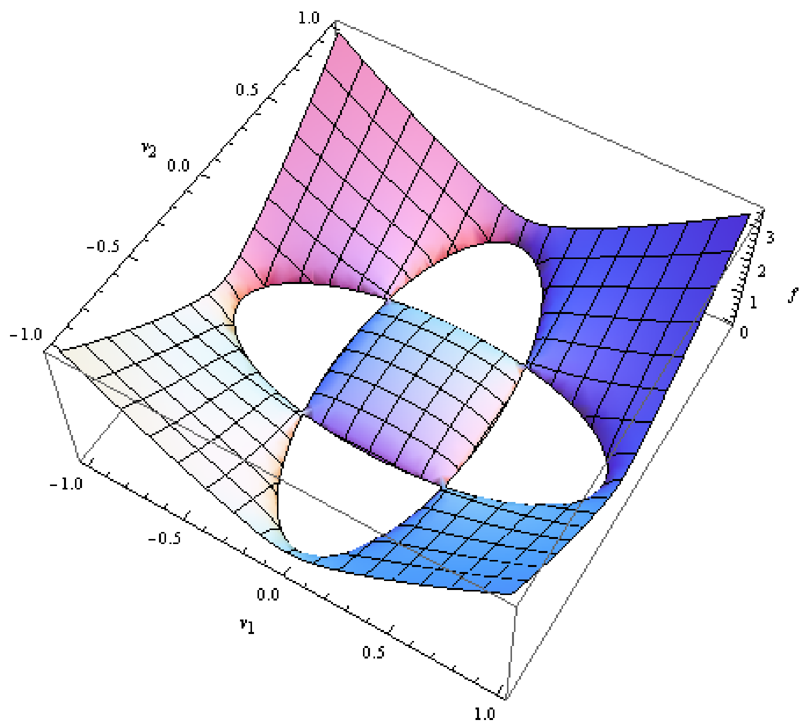

Figure 5.10: Figure representing the function f given by equation (5.28). The choice of the phase is $c = \frac{\pi}{2}$, i.e. $a = \cos\frac{c}{2} = \frac{1}{\sqrt{2}}$. It can be seen that the non-plotted (imaginary) part is the same as for the determinant of the Hessian matrix in the figure (5.3).

give us the answer. The interface between the real and the imaginary function is given by two ellipses described by the equations

$$
\begin{aligned}
E_1: \quad & v_1^2 \frac{2(2-a^2-2\sqrt{1-a^2})}{a^2(1-\sqrt{1-a^2})} + v_2^2 \frac{2}{1-\sqrt{1-a^2}} = 1 \\
E_2: \quad & v_1^2 \frac{2(2-a^2+2\sqrt{1-a^2})}{a^2(1+\sqrt{1-a^2})} + v_2^2 \frac{2}{1+\sqrt{1-a^2}} = 1.
\end{aligned} \tag{5.30}
$$

The intersection of the ellipses $E_{1,2}$ is given by

$$
v_2^{intersection} = \pm\sqrt{\frac{a^2(1+2v_1^2) - 4v_1^2 - (a^2-4v_1^2)\sqrt{(1-a^2)}}{2a^2}} \tag{5.31}
$$

and its interior points are real. If the region covered by the central real part of the functions f and $\det H$ correspond to the region covered by the quantum walk, then the intersection of the ellipses (5.31) have to correspond to the velocities that appears on the boarder of the region covered by the walk. These are the velocities of the smaller peaks given by the equations (5.21). The question is, if the intersection truly corresponds to those velocities. By substituting $v_1^{SP_{phase}}$ from equation (5.21) for the variable v_1 from equation (5.31) we truly obtain that

$$
v_2^{intersection} = v_2^{SP_{phase}}. \tag{5.32}
$$

In the figure (5.11) the ellipses $E_{1,2}$ from equation (5.30) with marked intersection (5.31) are given. It is for the phase $c = \frac{\pi}{2}$ i.e. $a = \frac{1}{\sqrt{2}}$. The important velocities are as in figure (5.2) for the velocities and the same phase ticked.

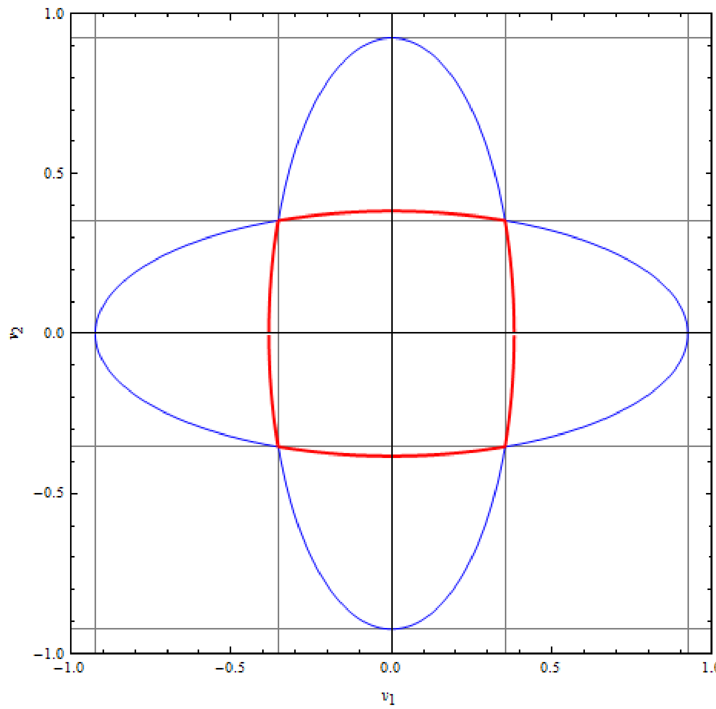

Figure 5.11: The ellipses $E_{1,2}$ from equation (5.30). The intersection given by equation (5.31) is represented by the thick red line. The phase of the walk $c = \frac{\pi}{2}$, i.e. $a = \cos\frac{c}{2} = \frac{1}{\sqrt{2}}$. The grid lines illustrates the velocities of the highest probability peaks and its location is $v_{1,2} = \pm\frac{1}{2}\frac{1}{\sqrt{2}}$.

Conclusion

It is known that the three-state Grover walk on a line exhibits the localization effect, the probability distribution has extra peak at the origin. We presented its generalization, one-parameter family of Grover walks, which is by the continuous transition between the Grover matrix and the permutation matrix formed. The Grover walk has three probability peaks. The central one does not move, but there are other two peaks traveling to the left and right with increasing number of steps.The generalized walk depends on the phase parameter $c \in (0, \pi)$. The family of walks contains the Grover walk as well, it is for $c = 0$. The shape of the probability distribution does not change. The localizing non-moving peak at the origin is preserved. The two remaining peaks travel with the group velocities that slow down with increasing c. The Grover walk is the fastest one from this family of localizing walks.

The Grover walk on the square lattice also exhibits the localization effect. In two dimensions, its probability distribution has two more peaks. Except the central one we can find four moving symmetrically distributed peaks. The probability distribution of the walk forms a circle. We presented two generalization of this walk. The first, inspired by [6], depends of the parameter $p \in (0, 1)$, where the choice $p = \frac{1}{2}$ leads to the Grover walk. The walk deforms the probability distribution into the ellipse, nevertheless the central peak and four remaining peaks are still observed. The group velocities of the highest moving probability peaks are determined by the parameter p. The second generalization of the Grover walk in two dimensions is based on the same principle as in the one-dimensional case. The continuous transition between the 4×4 Grover matrix and the permutation matrix give us the generalization dependent on the phase $c \in (0, \pi)$. The choice of $c = 0$ is equal to the Grover walk. The probability distribution is formed by the intersection of the two ellipses that differ on the factor $a = \cos \frac{c}{2}$. The central peak is preserved and the four remaining peaks are symmetrically distributed around the central one. Moreover, in contrast to the previous cases, the velocities on the whole probability boundary can be calculated. The four highest peaks are only the part of the boundary, the rest of it is formed by smaller (but significant) probability peaks.

In each chapter, when appropriate, we describe the wave-packet propagation using the concept of group velocity. This representation allowed us to find additional interesting properties of the walk.

The thesis presents new families of localizing coins for one and two dimensional walks. It is certainly worth to investigate whether these are the only possible walks or other classes can be found, especially in higher dimensions.

Appendix A

Asymptotic of integrals

For an easier treatment of the time evolution equation of the quantum walk we use the Fourier transformation. We replace the spatial variable by the more convenient momentum variable. However, we want the solution in the position variable. Therefore, we use the inverse Fourier transformation. The solution of the time evolution equation then has the form

$$I(t) = \int g(k) e^{itf(k)} dk, \quad f(t) \in \mathbb{R}. \tag{A.1}$$

This integral is called a generalized Fourier integral. Naturally we are interested in its asymptotic time behavior. There is a well-developed theory of the asymptotic expansion of Fourier integrals which gives us effective tools how to work with them and allows us to express the long time behavior as powers of time t. According to [3], the method of stationary phase asserts that the major contribution to the integral (A.1) comes from points where $f(k)$ has a vanishing derivative.

In the following we briefly review the fundamentals of the method of stationary phase for one and two dimensional integrals.

A.1 Method of stationary phase for one-dimensional integrals

The probability amplitude of the quantum walk on a line is given by the one-dimensional Fourier integral. Its asymptotic behavior is determined by the properties of the stationary points of the phase. Let us look in more detail into the possible cases.

A.1.1 No stationary point

Assume that there is no stationary point it the interval $\langle a, b \rangle$. Integration by part for large time.

$$I(t) = \left[\frac{g(k)}{itf'(k)} \right]_{k=a}^{k=b} - \frac{1}{it} \int_a^b \frac{d}{dk} \frac{g(k)}{f'(k)} e^{itf(k)} dk. \tag{A.2}$$

From the Riemann-Lebesgue lemma the second component of the (A.2) asymptotically decreases faster than 1/t. Therefore for $t \to \infty$ we find

$$I(t) \sim \left[\frac{g(k)}{itf'(k)} \right]_{k=a}^{k=b}. \tag{A.3}$$

We see that the decrease of the integral is proportional to $1/t$.

A.1.2 Simple stationary point

We cannot use integration by part, if there exist such a point $c \in \langle a, b \rangle$, where $f'(c) = 0$ (*stationary point*). When there exist stationary points, the Fourier integral must still vanish for long time from the Riemann-Lebesgue lemma, but the integrand oscillates slower near the stationary point. For this reason the integral decrease less rapidly and the leading term in the asymptotic behavior of the integral is constituted by the stationary point neighborhood.

Consider there is only one stationary point on (a, b). Without loss of generality we can consider stationary point as a, since every integral can be rewritten as a sum of integrals with stationary point on its boundary. Assume $f(a)$ is a minimum on the given interval. Then according to [4] we decompose $I(t)$ into two terms

$$I(t) = \int_a^{a+\epsilon} g(k) e^{itf(k)} dk + \int_{a+\epsilon}^b g(k) e^{itf(k)} dk, \quad t \to \infty. \tag{A.4}$$

The second term in the previous equation has no stationary point in the integration range. Hence it decreases as $1/t$ for large t and does not establish the leading behavior. Therefore we can exclude it. Since ϵ is a small positive number we can replace $g(t)$ with $g(a)$, and make the second order of the Taylor expansion of $f(k)$ around the stationary point a. It holds $f'(a) = 0$ and we obtain

$$I(t) \sim g(a) \int_a^{a+\epsilon} e^{it(f(a) + \frac{f''(a)}{2}(k-a)^2)} dk, \quad t \to \infty. \tag{A.5}$$

Now we replace ϵ by ∞ and substitute $x = (k - a)$

$$I(t) \sim g(a)e^{itf(a)} \int_0^{\infty} e^{it\frac{f''(a)}{2}x^2} dx, \quad t \to \infty. \tag{A.6}$$

After the substitution (note $f''(a) > 0$)

$$y = \sqrt{\frac{tf''(a)}{2}}x \tag{A.7}$$

we obtain

$$I(t) \sim g(a)\sqrt{\frac{\pi}{2tf''(a)}}e^{i(tf(a)+\pi/4)}, \quad t \to \infty. \tag{A.8}$$

Similarly, if $f(a)$ is a maximum, i.e. $f''(a) < 0$, then

$$I(t) \sim g(a)\sqrt{\frac{\pi}{2t|f''(a)|}}e^{i(tf(a)-\pi/4)}, \quad t \to \infty. \tag{A.9}$$

As we can see from equations (A.8) and (A.9), if the stationary point has non-zero second derivative, i.e. $f'(a) = 0, f''(a) \neq 0$, then for $t \to \infty$ the integral $I(t)$ behaves like reciprocal square root of time

$$I(t) \sim \frac{1}{t^{1/2}}. \tag{A.10}$$

A.1.3 Higher-order stationary points

The calculation can be generalized for any number of zero valued derivatives. If $f(t)$ is flatter, then the integral $I(t)$ decreases less rapidly for $t \to \infty$. Consider the stationary point c on the given interval, provided that $f'(c) = f''(c) = 0$ and $f'''(c) \neq 0$ than $I(t) \sim 1/t^{1/3}$. Similarly, let $p \in \mathbb{N}$, such as $f'(c) = ... = f^{(p-1)}(c) = 0$ and $f^{(p)}(c) \neq 0$ then $I(t) \sim 1/t^{1/p}$. Point c is called a stationary point of the order $p - 1$. To verify this claim we repeat the same procedure as in equations (A.6)-(A.9). Let us consider again boundary stationary point a, where $f(a) \neq 0, \quad f'(a) = ... = f^{(p-1)}(a) = 0$ and $f^{(p)}(a) \neq 0, \quad p \in \mathbb{N}$. After the decomposition of the integral on two terms as in (A.4) and exclusion of the second therm with no stationary point in the integration range we replace $g(k)$ by $g(a)$ and make Taylor expansion of $f(k)$ around the stationary point a. Thus, we find

$$I(t) \sim g(a) \int_a^{a+\epsilon} e^{it(f(a)+\frac{f^{(p)}(a)}{p!}(k-a)^p)} dk, \quad t \to \infty. \tag{A.11}$$

After replacing of ϵ by ∞ and substitution $x = (k - a)$ we obtain

$$I(t) \sim g(a)e^{itf(a)} \int_0^\infty e^{it\frac{f^{(p)}(a)}{2}x^p} dx, \quad t \to \infty. \tag{A.12}$$

To evaluate this integral we rotate the x-axis by an angle $\pm\pi/2p$. The sign depends on the value of $f^{(p)}(a)$, $+$ sign for $f^{(p)}(a) > 0$, $-$ sign for $f^{(p)}(a) < 0$. We make a substitution

$$x = e^{\pm i\pi/2p} \left(\frac{p!y}{t|f^{(p)|}(a)} \right)^{1/p}, \tag{A.13}$$

which leads us to the result

$$I(t) \sim g(a)e^{i(tf(a) \pm \pi/2p)} \left(\frac{p!}{t|f^{(p)}(a)|} \right)^{1/p} \frac{\Gamma(1/p)}{p}, \quad t \to \infty. \tag{A.14}$$

We find that the integral behaves like $1/t^{1/p}$ for large t.

A.2 Double integral

For the probability amplitude of the two-dimensional quantum walk we obtain, after the inverse Fourier transformation back to the position variables, integral in the form

$$I(t) = \iint\limits_D g(x, y)e^{itf(x,y)} dxdy, \quad f(x, y) \in \mathbb{R}, \ t > 0, \tag{A.15}$$

where D is a bounded domain. The entire chapter in [3] is dedicated to the asymptotic behavior of integrals of this type. Let us mention only few of the results. Assume that f and g are smooth function. Again as in the one-dimensional case, the main significant contributions for large parameter t come from critical points. The critical points comprise stationary points of the function f on D or its boundary ∂D or points on the ∂D where it has a discontinuously turning tangent.

A.2.1 Local extrema

Now we look at the stationary points. Let $(0,0)$ be the stationary point of $f(x,y)$. We denote the partial derivatives evaluated at the stationary point by

$$f_{ij} = \left.\frac{\partial^{i+j} f}{\partial x^i \partial y^j}\right|_{(0,0)} . \tag{A.16}$$

The expansion around the stationary point the function $f(x,y)$ takes the form

$$f(x,y) = f_{00} + f_{11}xy + f_{20}x^2 + f_{02}y^2 + ... = f_{20}x^2 + f_{02}y^2 + ... \tag{A.17}$$

Without loss of generality we can assume $f_{00} = 0$. Now we rewrite the equation (A.17) and make several substitution

$$f(x,y) = f_{20}x^2(1 + p(x,y)) + f_{02}y^2(1 + q(x,y)) = f_{20}u^2 + f_{02}v^2, \tag{A.18}$$

where $u = (1 + p(x,y)),\ v = (1 + q(x,y))$. Subsequently substitute functions in integral (A.15)

$$G(u,v) = g(x,y)\frac{\partial(x,y)}{\partial(u,v)}, \quad F(u,v) = f_{20}u^2 + f_{02}v^2. \tag{A.19}$$

Afterwards, the integral (A.15) turns into

$$I(t) \sim \iint\limits_D G(u,v)e^{itF(u,v)}dudv, \quad F(u,v) \in \mathbb{R},\ t > 0,\ t \to \infty. \tag{A.20}$$

Further

$$G(u,v) = \sum_{m,n=0}^{\infty} G_{ij}u^i v^j, \quad G_{00} = g_{00}. \tag{A.21}$$

We do not go into the details of the following calculation and write only the resulting formula. For more information about the method see [3]. The asymptotic behavior of the integral is given by

$$I(t) \sim \frac{1}{\sqrt{f_{02}f_{20}}} \sum G^*_{2m,2n} e^{i\pi(m+n\pm1)/2} \frac{\Gamma(m+1/2)\Gamma(n+1/2)}{t^{m+n+1}}, \ t \to \infty. \tag{A.22}$$

The sign in the exponent depends on whether the stationary point is minimum (*plus sign*) or maximum (*minus sign*). The coefficients G^*_{ij} reads

$$G^*_{ij} = \frac{G_{ij}}{f_{20}^{i/2} f_{02}^{j/2}}. \tag{A.23}$$

We see that the integral decays like $1/t$.

A.2.2 A continuous curve of stationary points

Consider that the domain D contains a curve of stationary points. Assume the validity of the following conditions

- The domain D contains a curve γ from C^∞ and $\nabla f = (0,0)$ on the curve, $\nabla f \neq (0,0)$ on $D \backslash \gamma$. Further γ has no loops, and the derivatives $f_{xx} + f_{yy} \neq 0$ on γ.
- Let parametrize the curve γ by its arc length s. Denote $x = \xi(s),\ y = \eta(s),\ 0 \leq s \leq L$, where L is the length of γ. Let Γ be the boundary of the domain D. If $A = (\xi(0), \eta(0)),\ B = (\xi(L), \eta(L)$, then $A, B \in \Gamma$. Moreover $A \neq B, (\xi(s), \eta(s)) \notin \Gamma$ for $0 < s < L$.
- At A and B, γ and Γ are not tangent to each other.

Theorem: Under the above conditions we obtain

$$I(t) \sim \sum_{s=0}^{\infty} b_s t^{-\frac{s+1}{2}}, \quad t \to \infty \tag{A.24}$$

and coefficients b_s are independent of t.

The above theorem is the main result for the asymptotic behavior. We will show how to get the result only briefly, for more precise derivation see [3]. The first condition implies that $f = f_0$ is constant on γ. Thus we can suppose that $f_0 = 0$ without loss of generality. It should be assumed that the functions f, g are extended to C^∞ in some open neighborhood of $\bar{D}$ and ξ, η are extended to C^∞ in some open neighborhood of $[0, L]$. Now we can define a transformation $M : (s, p) \to (x, y)$

$$x = \xi(s) - p\eta'(s), \quad y = \eta(s) + p\xi'(s). \tag{A.25}$$

The absolute value of p represents the distance from (x, y) to γ and from s as the arc length of the curve γ follows that $\xi'(s) + \eta'(s) = 1$. The Jacobian of the transformation M is

$$\frac{\partial(x, y)}{\partial(s, p)} = 1 + p(\xi''(s)\eta'(s) - \xi'(s)\eta''(s). \tag{A.26}$$

It can be shown that the transformation M is one-to-one on the rectangle. Thus there exist suchϵ, δ positive that M is one-to-one in $Q_\delta = (-\epsilon, L + \epsilon) \times (-\delta, \delta)$. Changing the variables $(x, y) \to (s, p)$ in the integral $I(t)$ we obtain

$$I(t) = \iint\limits_{R_\delta} G(s, p) e^{itF(s,p)} ds dp, \tag{A.27}$$

where $R_\delta = M^{-1}(D_\delta)$ and $F(s, p) = f(x, y),\ G(s, p) = g(x, y)\frac{\partial(x,y)}{\partial(s,p)}$. Assume δ sufficiently small that R_δ in Q_δ can be determined by equations $s = a(p),\ s = b(p)$. Then we can write

$$I(t) = \int_{a(p)}^{b(p)} \int_{-\delta}^{\delta} G(s, p) e^{itF(s,p)} ds dp. \tag{A.28}$$

Now we list some facts resulting from the conditions above and from the transformation M. From the first condition follows $\nabla F(s, 0) = (0, 0),\ 0 \leq s \leq L$, thus

$$\frac{\partial^{k+1} F}{\partial s^{k+1}}(s, 0) = \frac{\partial^{k+1} F}{\partial s^k \partial t}(s, 0) = 0,\ k \geq 0,\ s \in [0, L]. \tag{A.29}$$

This relation shows that $F(s, 0)$ is constant, without loss of generality we can put $F(s, 0) = 0$. Moreover from equation (A.29) we obtain the following expansions

$$\begin{aligned}
F(s, p) &= F_{pp}(s, 0)\frac{p^2}{2} + F_{ppp}(s, 0)\frac{p^3}{6} + O(p^4) \\
F_s(s, p) &= F_{pps}(s, 0)\frac{p^2}{2} + F_{ppps}(s, 0)\frac{p^3}{6} + O(p^4) \\
F_p(s, p) &= F_{pp}(s, 0)p + F_{ppp}(s, 0)\frac{p^2}{2} + O(p^3) \\
F_{p,p}(s, p) &= F_{pp}(s, 0) + F_{ppp}(s, 0)p + O(p^2).
\end{aligned} \tag{A.30}$$

Since $F(s, p) = f(x, y)$ we have

$$F_{pp} = f_{xx}\eta'^2 + f_{yy}\xi'^2 - 2f_{xy}\xi'\eta'. \tag{A.31}$$

The condition $\xi'^2 + \eta'^2 = 1$ gives

$$F_{pp} = f_{xx} + f_{yy} - (f_{xx}\eta'^2 + f_{yy}\xi'^2 + 2f_{xy}\xi'\eta'), \tag{A.32}$$

also

$$F_{pp}(s,0) = f_{xx}(\xi(s),\eta(s)) + f_{yy}(\xi(s),\eta(s)) - \frac{d^2}{ds^2}f(\xi(s),\eta(s)),\ 0 \le s \le L. \tag{A.33}$$

Since the function f is constant on the curve γ we have

$$F_{pp}(s,0) = f_{xx}(\xi(s),\eta(s)) + f_{yy}(\xi(s),\eta(s)),\ 0 \le s \le L. \tag{A.34}$$

The first condition at the beginning gives non-zero $F_{pp}(s,0)$, without loss of generality $F_{pp}(s,0) > 0$ can be supposed. Let us choose δ sufficiently small, thus we can assume also $F_{pp}(s,p) > 0$ in R_δ. Now the relations

$$\begin{aligned} F(s,p) &> 0 \\ sgn F_p(s,p) &= sgn\ p, \quad (s,p) \in R_\delta,\ p \ne 0. \end{aligned} \tag{A.35}$$

can be deduced. We would like to transform the integral (A.28) to a one-dimensional Fourier integral. To do that, we have to define a second transformation $N : (s,p) \to (w,z)$ as follows:

$$\begin{aligned} w &= s \\ z^2 &= F(s,p);\ sgn\ z = sgn\ p. \end{aligned} \tag{A.36}$$

The Jacobian of this transformation is

$$\frac{\partial(w,z)}{\partial(s,p)} = \frac{F_p(s,p)}{2\sqrt{F(s,p)}sgn\ p} \to \sqrt{\frac{F_{tt}(s,0)}{2}},\quad t \to 0,\ 0 \le s \le L. \tag{A.37}$$

Note that the mapping is one-to-one on R_δ. The integral (A.28) now has form

$$I(t) = \int_{-\rho}^{\rho} e^{itz^2}\Phi(z)dz, \tag{A.38}$$

where

$$\rho^2 = sup\{F(s,p) : (s,p) \in R_\delta\},$$

$$\Phi(z) = \int_{\gamma(z)} G(s,p)\frac{2z}{F_p(s,p)}dw. \tag{A.39}$$

The curve is given by $\gamma(z) = \{w : (w,z) = N(s,p); (s,p) \in R_\delta\}$. From the definition of $G(s,p)$ the function $\Phi(z)$ vanishes for $z \to \pm\rho$. The asymptotic behavior of $I(t)$ is then determined by the behavior of the function $\Phi(z)$ near zero. Rewrite

$$I(t) = I^+(t) + I^-(t), \tag{A.40}$$

where

$$I^\pm(t) = \int_0^\rho e^{itz^2} \Phi(\pm z) dz. \tag{A.41}$$

For sufficiently small z we can write

$$\Phi(z) = \int_{\alpha z^2}^{\beta z^2} G(s,p) \frac{2z}{F_p(s,p)} dw. \tag{A.42}$$

Repeating integration by parts we obtain

$$I^\pm(t) = 1/2 \sum_{s=0}^{n-1} \frac{1}{s!} \Gamma\left(\frac{s+1}{2}\right) e^{i(s+1)\pi/4} (\pm 1)^s \Phi^{(s)}(0^\pm) t^{-\frac{s+1}{2}} + O(t^{-\frac{n+1}{2}}). \tag{A.43}$$

This implies the statement of the theorem.

Bibliography

[1] N. Inui, N. Konno, E. Segawa: *One dimensional three state quantum walks*. Phys. Rev. E 72, 056112 (2005).

[2] M. Štefaňák, T. Kiss, I. Jex: *Recurrence of biased quantum walks on a line*. New Journal of Physics 11, 043027 (2009).

[3] R.Wong: *Asymptotic Approximations of Integrals*. SIAM, (2001)

[4] C. M. Bender, S. A. Orszag: *Advanced Mathematical Methods for Scientists and Engineers*. International Series in Pure and Applied Mathematics. McGraw-Hill, Inc., New York, (1978)

[5] K. Watabe, N. Kobayashi, M. Katori and N. Konno: *Limit distributions of two-dimensional quantum walks*. Phys. Rev. A 77, 062331 (2008).

[6] N. Inui, Y. Konishi and N. Konno: *Localization of two-dimensional quantum walks*. Phys. Rev. A 69, 052323 (2004).

[7] M. Štefaňák, I. Bezděková and I. Jex: *Continuous deformations of the Grover walk preserving localization*. Eur. J. Phys. D (2012), accepted for publication.

[8] J. Kempe: *Quantum random walks: and introductory overview*. Contemp. Phys. 44, 307.

[9] A. Kempf and R.Portugal: *Group velocity of discrete-time quantum walks*. Phys. Rev. A 79, 052317 (2009).